Adaptive Sampling: Efficient Search Schemes under Resource Constraints

Eran Bashan, Raviv Raich, and Alfred O. Hero III, *Fellow, IEEE*

October 24, 2007

Abstract

The field of adaptive sampling has generated a lot of excitement in the signal processing community. It was shown that a certain class of inhomogeneous signals can be reconstructed with far fewer samples than required by traditional sampling methods. However, this class does not cover interesting signals for which adaptive sampling methods can be used. Applications such as target monitoring involve both detecting targets locations, in a given domain, and estimating their parameters. Generally, reconstructing the complete signal is equivalent to estimating nuisance parameters. We consider the problem of reconstructing an unknown region of interest (ROI) within a given signal. We introduce a novel cost function, trading the proportion of efforts distributed to the unknown ROI and its complement. We show that minimizing our cost implies reducing both error probability over the unknown ROI and mean square error (MSE) in estimating the ROI content. Two solutions to the effort allocation problem, subject to a total effort constraint, are derived distributing search efforts in a data dependant manner. Our adaptive measuring schemes sequentially concentrate search efforts to an estimated ROI, thus embedding the detection task into the data acquisition process. Asymptotic analysis shows that this estimated ROI converges to the true ROI. We evaluate performance and compare the two novel search policies to an exhaustive search for both detection and estimation tasks. We show that our method both outperforms an exhaustive search and approaches the theoretical limits of the possible performance gain in terms of MSE reduction. An illustrative example of our method in the context of target detection and estimation is also provided.

I. Introduction

Adaptive sampling has been an exciting research topic in the signal processing community in recent years. Using spatial properties of signals, it was shown that a signal may be reconstructed

from far fewer samples than required by traditional sampling scheme [1]–[5]. This paper considers the problem of detecting and estimating the content of an unknown region of interest (ROI) within a signal. In many applications a signal is first completely reconstructed, then scanned to extract a ROI, examples include: target detection and classification, computer aided diagnostic, and screening. Our goal is to embed the detection process into the data acquisition process under resource constraints.

In a reconnaissance mission, active radar may be used to image a given scene. A typical system is designed to detect targets exceeding a minimal profile. This minimal target profile dictates the scan parameters such as the energy level the radar transmits and the scan time duration. Moreover, targets usually occupy a small section of the scanned area, namely the ROI. Most systems consider exhaustive search with equal energy allocation[1] to spread sensitivity over all locations. As a result, a relatively large portion of the energy is allocated outside the ROI. This excess energy could be used to better illuminate the ROI. Furthermore in surveillance applications, by deploying energy over an unknown area the searcher risks exposure. Reducing the scan energy outside the ROI reduces exposure risks.

As another application, consider the task of early detection of tumors using medical imaging. Early detection implies a small tumor and usually no *a priori* knowledge about the tumor location exists. We consider the area containing the tumor as an unknown ROI. Often, safety constraints limit the total energy used in a specific scan, e.g., CT and X-rays expose patients to unsafe radiation. There are two questions to answer: *a*) where are tumors located, i.e., detecting the unknown ROI. *b*) what kind of tumors does the ROI contain, i.e., estimating the ROI content. This classic combined detection/estimaiont task suggests using adaptive sampling scheme to improve both detection and estimation performance.

Previous work on adaptive sampling concentrated at inhomogeneous signals [1]–[5]. We consider general signals restricted only to have a small ROI[2]. Such signals may be thought of as sparse. Most of the existing work on sparse signals considers post processing tasks [6]–[13], while we utilize the 'sparsity' during the data acquisition phase. Resource allocation without the

[1]We define exhaustive search policy as a search policy where all possible locations (cells) are searched in an exhaustive manner with equal effort allocated to each cell. This is different from exhaustive enumeration of all possible search policies.

[2]Formally stated, the ratio between the support of the ROI to the support of the entire signal has to be small.

notion of ROI was considered in [14]–[16]. Resource allocation in a somewhat restricted manner is discussed in [17]–[19] in the context of sensor management where the main concern is where to point the sensor next. Search theory research produced a great deal of work but most of it does not apply to the matter at hand, see [20] for a comprehensive survey. Finally, our results have some similarity to Posner's work on minimizing expected search time for finding a satellite lost in the sky [21]. See Section I-A for an extended literature review.

In this work, we focus on adaptively concentrating search efforts at an estimated ROI. This process yields a nonuniform, data dependent, measuring scheme. The main contributions of this work is two-fold: (i) we formulate a novel framework for the problem of effort allocation leading to solutions that minimize both the Chernoff bound on error probability and the *Cramér-Rao* bound on estimating the content of the ROI, for certain cases. (ii) we provide a two-step optimal and a suboptimal adaptive effort allocation policies with respect to (w.r.t.) our cost function. The optimal policy is given in closed form and follows the same logic leading to the water-filling algorithm. The suboptimal policy is a straight forward mapping from the data space to the search space. Both policies outperforms an exhaustive search scheme for post processing tasks, such as detection and estimation. Moreover, an asymptotic (high SNR) performance analysis is given and we show that the estimated ROI converges to the true ROI and performance gain approaches the theoretical limit inversely proportional to the sparsity of the problem.

The rest of this paper is organized as follows: In Section I-A, we review related work. Section II formally states the problem and introduces our cost function. In Section III, we present optimal and suboptimal solutions for the effort allocation problem. Section IV includes thorough performance evaluation of the two policies as compared to an exhaustive search policy for both detection and estimation tasks. An illustrative imaging example of our methods using synthetic aperture radar data is given in Section V. Finally, we conclude and point to future work in Section VI.

A. Related work

Most of the previous work on adaptive sampling[3] has concentrated on estimating functions in noise. Castro et al. [1] present asymptotical analysis and shows that for piecewise constant functions adaptive sampling methods can capitalize on spatial properties of the function. By focusing samples to the estimated vicinity of the boundaries, adaptive sampling methods yield nearly optimal convergence rate, in terms of estimation mean square error (MSE). It is also shown that for spatially homogeneous functions adaptive sampling has no advantages over passive sampling. Nowak et al. [2], Castro et al. [3], and Willett et al. [4] consider different applications characterized by spatially inhomogeneous functions, for which adaptive sampling methods can be efficiently used. In [5], Castro et al. show that for certain classes of piecewise constant signals *compressed sensing* is as efficient as adaptive sampling, in terms of the estimation error convergence rate. In our work, we are not interested in estimating the entire function but rather finding an ROI and estimate its content.

Although we consider homogenous signals, we assume that the support of the ROI is small as compared to the entire support of the signal. We refer to such signals as sparse. Sparsity is used in a variety of applications: signal compression, reconstruction, approximation, source separation and localization, and target tracking or detection [6]–[13]. Most of the related research considers post processing tasks. Matching pursuit [6] use a greedy algorithm to select base elements from the dictionary. Algorithms like FOCUSS [7] use sparsity to reconstruct a signal from limited samples. Nafie et al. [8] address the problem of subset selection. Wohlberg [9] provides reconstruction error bounds for several sparse signal bases. Sparse solutions using l_1 penalty are used in [10] to improve performance in direction-of-arrival estimation. Tropp lays theoretical foundations for convex relaxation techniques for sparse optimization problems [11]. Escoda et al. incorporate *a priori* knowledge of the signal structure to compensate for a potentially coherent dictionary [12]. An algorithm that adapts a dictionary to a given training set is given in [13]. In our work, we would like to utilize the sparsity during the data acquisition phase as a pre-processing task.

Resource allocation is also considered in the context of sensor scheduling/management [17]–

[3]In the literature this is also referred to as active learning or active sampling.

[19]. In sensor management, an agile array of sensors is used to scan a certain domain[4]. At each time step, one chooses which grid point (cell) to search next and in what mode. Generally, a number of existing targets need to be tracked while new targets are being looked for. Kastella looks at such task under low signal to noise ratio (SNR) [17]. He introduces the discrimination gain based on the Kullback-Leibler information to quantify the usefulness of the next measurement. Using a myopic strategy, Kastella shows that pointing the sensor to the cell maximizing the discrimination gain decreases the probability of incorrectly detecting where a target is. Kreucher et al. show that integrating the sensor management algorithm with the target tracking algorithm via the posterior joint multi-target probability density (JMPD), allows to predict which measurement provides the most information gain, [18] and [19]. Our approach differs as we consider energy control in a continuous manner.

Adaptive energy allocation is addressed in [14]–[16]. Rangarajan et al. consider the problem of adaptive amplitude design for estimating parameters of an unknown medium under average energy constraints (fix energy constraints in [14]). They treat an N time-steps design problem and provide an optimal solution for the case of $N = 2$ in terms of minimizing estimation MSE. However, they do not consider the parameter vector of interest to be sparse and as a result only minor gains are possible. Using our method we show asymptotic gains in MSE inversely proportional to the sparsity of the scanned domain.

The field of *Search Theory* considers the following problem: a single target is hidden in one of Q boxes. Each box is also equipped with prior, detection, and false alarm probabilities. A desirable search policy maximizes the probability of correctly detecting the location of the target. For review of the problem and reference therein see [20]. From the earlier work of Kadane [22] on "whereabouts search" to a more recent work of Castanon [23] on "dynamic hypothesis testing", the question remains which cell to sample next in order to maximize the probability of detecting the location of the target. Castanon shows that a myopic strategy is optimal for certain noise characteristics. Although search theory has generated much research for more than six decades, most of the work has concentrated on searching one box at a time. In our case, we relax this stringent restriction. Song and Teneketzis [24] generalize the framework to a search

[4]We refer to the entire support of the signal as the scanned domain, which contains the ROI.

of m cells at each step. They derive two condition under which a search policy is optimal for either a fixed horizon K or for any horizon respectively. Most search theory literature considers independent measurements between neighboring cells and over time. This model enables an offline calculation of a compact static table listing the probability of detecting the target while searching a cell at a given time. In turns, the table is used to find an optimal search policy. Castanon extends this model and consider the case of dependent cells where the probability table is dynamically updated [23]. This is also the case in our work, although we introduce dependency between cells in a dual manner: over time and via a sparsity constraint.

To the best of our knowledge, Posner [21] was the first to consider searching more than one box at a time. He considers the problem of using a radar to locate a satellite lost in a region of the sky containing Q cells. His goal is to minimize the expected total search duration, and the idea is to search the cells where the satellite is most likely to be first. Assuming a uniform prior, the competing strategy exhaustively searches each cell for time t_1 with an expected search time of $t_1(Q+1)/2$. Posner suggests a preliminary search yielding a non-uniform posterior, followed by a search of all cells for a time t_1 in a descending likelihood order. For the preliminary search he allows to widen the radar beam and measure k cells for a time t in each measurement. Moreover, Posner allows to take as many preliminary searches as necessary. In his model, the detection probability increases in t and decreases in k. Posner shows that the optimal solution minimizing the expected search time takes a single preliminary search, in which $k = 1$ and t is small (i.e., to take a sneak peek at each cell) to create a posterior distribution then measure each cell again in the new order. It is interesting to note that even though we consider a different cost function our solution follows a similar approach. A portion of the search effort has to be uniformly allocated to all cells to generate a posterior distribution; however we use the posterior distribution to update the effort allocation for each cell.

In medical imaging, we are specifically interested in early detection of breast cancer tumors. About one out of every seven women will experience breast cancer over a 90-year life span. If detected at an early stage, the patient stands an excellent recovery chance. However, detecting early stage tumors is a hard task, especially among younger women. Microwave imaging technology provides high contrast between normal breast fatty tissue and tumors and is a promising imaging modality for this application [25]–[29]. Bond et al. [26] suggest an exhaustive search policy

for early detection of breast cancer. Although microwave energy is a non-ionizing radiation, it generates heat within the scanned tissue, which limits the energy level that can be safely used for a scan. Additionally, since this is an active radar system, the SNR depends on the amplitude of the transmitted signal. Hence, a search policy that would concentrate energy around region of interests should outperform an exhaustive search for a given total energy budget. We provide an illustrative example showing how our methods can be used to improve image quality over the ROI without exceeding safety limits, namely a total resource constraint, in Section V.

II. Problem formulation

Consider a discrete space $\mathcal{X} = \{1, 2, \ldots, Q\}$ containing Q cells and equipped with a probability measure P. Let Ψ be a subset of $\mathcal{X}$, i.e., $\Psi \subseteq \mathcal{X}$. We use Ψ to denote an ROI[5] in $\mathcal{X}$ and in the sequel Ψ will be assumed to be a random subset of $\mathcal{X}$. Let I_i be an indicator function of the ROI such that

$$I_i = \begin{cases} 1, & i \in \Psi \\ 0, & \text{Otherwise} \end{cases} \tag{1}$$

and $\{p_i = \Pr(I_i = 1)\}_{i=1}^{Q}$ is an associated set of prior probabilities. Let $\boldsymbol{I}_\Psi = [I_1, \ldots, I_Q]'$ be a vector corresponding to the set of all indicators and $(\cdot)'$ denotes the transpose operator. We say that the presence of a target affects cell i if $i \in \Psi$. Define the random vector $\boldsymbol{Y} : \mathcal{X} \to \mathbb{R}^Q$ and consider the conditional probability $p(\boldsymbol{Y}|\boldsymbol{I}_\Psi)$.

Consider a sequential experiment where cell i may be sampled T times. By sampling we mean that $\boldsymbol{y}(t)$, a realization of $\boldsymbol{Y}$, is observed at time t. Let the distribution $\lambda(i,t) \geqslant 0$ denote the search effort allocated to cell i at time t, with

$$\sum_{t=1}^{T} \sum_{i=1}^{Q} \lambda(i,t) = 1, \quad 0 \leqslant \lambda(i,t) \leqslant 1 \tag{2}$$

and $\{\lambda(i,t)\}$ is a mapping from past observations $\boldsymbol{y}_1, \ldots, \boldsymbol{y}_{t-1}$ to the probability simplex and is called an effort allocation policy, or equivalently, a search policy. We focus here on deterministic mapping λ, although in general random mapping can be considered if necessary. We assume

[5]Exact definition of the ROI is application dependent. In radar target localization it-may be sufficient if the ROI is the collection of all cells containing targets and target related phenomena, e.g., target shadows. In a medical imaging application, such as an early detection of breast cancer, seeing only the tumor is probably not enough. Therefore, in case of the latter, the ROI may be defined as the collection of all cells containing targets plus some neighboring cells.

that the 'quality' of the samples, e.g. measured in terms of information or inverse variance, is an increasing function of the allocated effort to the associated cell. In general, effort might be: time, computing power, complexity, cost, or energy, allocated to acquiring a particular cell location. Define the cumulative search effort allotted to cell i, as

$$\Lambda(i) = \sum_{t=1}^{T} \lambda(i,t). \tag{3}$$

Consider the following cost function

$$J(\Lambda) = \sum_{i=1}^{Q} I_i A(\Lambda(i)) + \sum_{i=1}^{Q} B(\Lambda(i)), \tag{4}$$

where $A(\cdot)$ and $B(\cdot)$ are decreasing functions that may depend on additional parameters. This restriction ensures that allocating more effort to cells reduces the over all cost. Note that our cost function (4) depends directly on the ROI via the summand of the first sum on the right hand side (r.h.s.) of (4). Choosing $B(\cdot) = 0$ requires focusing efforts onto the ROI to minimize (4). Setting $A(x) = \frac{2\nu-1}{x}$ and $B(x) = \frac{1-\nu}{x}$, with $\nu \in [\frac{1}{2}, 1]$, simplifies $J(\Lambda)$ to

$$J(\Lambda) = \sum_{i=1}^{Q} \frac{\nu I_i + (1-\nu)(1-I_i)}{\Lambda(i)}. \tag{5}$$

Minimizing this cost function concentrates ν of the total effort over the ROI Ψ and $(1-\nu)$ to its complement Ψ^c with ν being the dividing factor. Setting $\nu = 1$ focuses all the effort at the ROI, while $\nu = \frac{1}{2}$ results in an exhaustive effort allocation scheme, i.e., equal energy allocated to all cells inside and outside the ROI. Also, with $\nu = 1$ minimizing (5) has some very intuitive and appealing properties. For example, in the context of estimating a deterministic signal $\boldsymbol{\mu}$ in additive Gaussian noise, minimizing (5) is equivalent to minimizing the *Cramér-Rao* lower bound on $\mathrm{E}\{\sum_i I_i(\hat{\mu}_i - \mu_i)^2\}$, see Appendix I for details. In a sense, ν controls the tradeoff between learning on parameters of interest and learning on nuisance parameters.

In addition, consider a binary Gaussian hypothesis testing problem. Define the null hypothesis, $H_0(i)$, as $\mu_i = 0$, and the alternative, $H_1(i)$, as $\mu_i > 0$ with a prior probability $p = \Pr(H_1)$. Consider the task of deciding between the two hypothesis, $\forall i \in \Psi$. The probability of error, i.e., making the wrong decision, defined as $P_e = \Pr(\text{decide } H_0|H_1)p + \Pr(\text{decide } H_1|H_0)(1-p)$, can be broken into two parts: misdetect probability P_m over Ψ, and false alarm probability P_{fa} over Ψ^c. With $\nu = 1$, we show in appendix II that minimizing (5) is equivalent to uniformly minimizing the Chernoff bound on the probability of error P_m over the ROI. Setting $\nu = \frac{1}{2}$, most

of the energy is spread over Ψ^c, hence, minimizing (5) is equivalent to uniformly minimizing the Chernoff bound on P_{fa}. If $\nu \in (\frac{1}{2}, 1)$ we trade the two cases, either relaxing the upper bound on P_m or on P_{fa}. In section IV we corroborate this theory with simulation results. Measurement schemes derived from solutions to (5) are used to generate data as a pre-processing phase for both estimation and detection task. We show that our adaptive search scheme provides significant performance improvement for both estimation and detection.

Note that our cost function (4) is independent of time and depends only on the cumulative search effort allocation Λ. This is similar to a multi arm bandit (MAB) problem with a terminal/total reward function. The main difference to the MAB problem is that each action we take, namely $\lambda(i,t)$, affects the observation model. In a MAB problem, at each stage we choose 'which arm to pull', where here we also choose how 'hard' to pull the leaver. Pulling 'harder' yield a more informative observation.

Next, we provide an achievable lower bound on our cost function (5), derive an optimal effort allocation scheme, and define a performance gain function.

Lemma 1: The cost function (5) is lower bounded by

$$J(\Lambda) \geqslant \left[\sqrt{\nu}|\Psi| + \sqrt{1-\nu}(Q - |\Psi|)\right]^2. \tag{6}$$

Proof: For a nonnegative series $\{a_i\}$, Cauchy-Schwarz inequality provides

$$\left(\sum_{i=1}^{Q} \frac{a_i}{\Lambda(i)}\right)\left(\sum_{i=1}^{Q} \Lambda(i)\right) \geqslant \left(\sum_{i=1}^{Q} \sqrt{\frac{a_i}{\Lambda(i)}}\sqrt{\Lambda(i)}\right)^2. \tag{7}$$

Since $\sum_{i=1}^{Q} \Lambda(i) = 1$, (7) simplifies to

$$\sum_{i=1}^{Q} \frac{a_i}{\Lambda(i)} \geqslant \left(\sum_{i=1}^{Q} \sqrt{a_i}\right)^2. \tag{8}$$

Substituting $a_i = \nu I_i + (1-\nu)(1-I_i)$, i.e.,

$$a_i = \begin{cases} \nu, & i \in \Psi \\ (1-\nu), & i \in \Psi^c \end{cases}, \tag{9}$$

into the r.h.s. of (8) yields

$$\left(\sum_{i=1}^{Q} \sqrt{a_i}\right)^2 = \left[\sqrt{\nu}|\Psi| + \sqrt{1-\nu}(Q - |\Psi|)\right]^2. \tag{10}$$

Noting that on the l.h.s. of (8) we have $J(\Lambda) = \sum_{i=1}^{Q} \frac{a_i}{\Lambda(i)}$ completes the proof. ■

Lemma 2: The lower bound in *Lemma* 1 is achievable with a two-level effort allocation scheme, uniform over the ROI and uniform over its complement.

Proof: The equality in Cauchy-Schwarz inequality is achieved when $\sqrt{\frac{a_i}{\Lambda(i)}} = c\sqrt{\Lambda(i)}$ for all i. Utilizing the sum-to-one property of the distribution Λ provides $c = \sum_{i=1}^{Q} \sqrt{a_i}$, thus

$$\Lambda(i) = \frac{\sqrt{a_i}}{\sum_{j=1}^{Q} \sqrt{a_j}}. \tag{11}$$

Substituting (9) into (11), the lower bound in *Lemma* 1 is achieved for

$$\Lambda_o(i) = \begin{cases} \frac{\sqrt{\nu}}{\sqrt{\nu}|\Psi| + \sqrt{1-\nu}(Q-|\Psi|)}, & i \in \Psi \\ \frac{\sqrt{1-\nu}}{\sqrt{\nu}|\Psi| + \sqrt{1-\nu}(Q-|\Psi|)}, & i \in \Psi^c \end{cases}. \tag{12}$$

Note that

$$J(\Lambda_o) = \sum_{i \in \Psi} \frac{\nu}{\Lambda_o(i)} + \sum_{i \in \Psi^c} \frac{1-\nu}{\Lambda_o(i)}, \tag{13}$$

and therefore

$$J(\Lambda_o) = \left[\sqrt{\nu}|\Psi| + \sqrt{1-\nu}(Q - |\Psi|)\right]^2, \tag{14}$$

which is exactly the r.h.s. of (6). This completes the proof. ■

Discussion: We would like to point out the potential gains in terms of our cost function (5). As previously mentioned, for $\nu = \frac{1}{2}$ in (12) the optimal effort allocation scheme is the uniform effort allocation $\Lambda_U(i) = \frac{1}{Q}$. For a general ν, the cost (5) associated with Λ_U is

$$J(\Lambda_U) = Q\left[\nu|\Psi| + (1-\nu)(Q - |\Psi|)\right], \tag{15}$$

with the two special cases of

$$J(\Lambda_U) = \begin{cases} \frac{Q^2}{2}, & \nu = 0.5 \\ Q|\Psi|, & \nu = 1 \end{cases}. \tag{16}$$

Since Λ_U does not offer any adaptivity, any good adaptive effort allocation scheme Λ should result in $J(\Lambda) \leqslant J(\Lambda_U)$. Therefore, we define the performance gain in [dB] as

$$G(\Lambda) = -10 \log \frac{J(\Lambda)}{J(\Lambda_U)}. \tag{17}$$

For $\nu = 1$, $J(\Lambda_o) = |\Psi|^2$ and thus the optimal gain is

$$G(\Lambda_o) = -10 \log \frac{|\Psi|}{Q}. \tag{18}$$

Define $p^* = \frac{|\Psi|}{Q}$, then $p^* \to 0$ provides $G(\Lambda_o) \to \infty$. Consequently, a good sampling method should yield large gains in a sparse setting, i.e., when p^* is small and only a few cells are in the ROI. In the following, we will develop a sampling method that aims at attaining these gains.

Taking the derivative of the r.h.s. in (6) w.r.t. ν, it can be shown that $J(\cdot) \geqslant |\Psi|^2$ for all $\nu \in [\frac{1}{2}, 1]$ and $\frac{|\Psi|}{Q} \leqslant \frac{1}{2}$ (see Appendix III). In other words, if $\frac{|\Psi|}{Q} \leqslant \frac{1}{2}$ the optimal gain is achieved by Λ_o for $\nu = 1$. Unfortunately, Λ_o is not a feasible policy since we do not know the location of the ROI in advance. Nevertheless, our goal is to derive an effort allocation policy $\lambda(i,t)$ that concentrate search efforts into an estimated ROI.

In this paper, we restrict our attention to minimizing the expected value of (5). This probabilistic setting utilizes the conditional distribution $p(\boldsymbol{Y}|\boldsymbol{I}_\Psi)$ in our model. Assuming we observe realizations of $\boldsymbol{Y}$, our goal is to find a search effort distribution[6]

$$\hat{\lambda}(i,t) = \arg\min_{\lambda(i,t)} \mathrm{E}\left\{ \sum_{i=1}^{Q} \frac{\nu I_i + (1-\nu)(1-I_i)}{\Lambda(i)} \right\}, \tag{19}$$

where $\Lambda(i)$ is given by (3). Next, we reformulate this problem in the context of energy allocation with a total energy constraint.

A. Energy allocation with energy constraint

Consider a stationary radar target localization in the presence of noise. We assume that a radar transmits energy in some known beam pattern to probe a collection of cells. We further assume that measuring is done under an energy constraint, and that observations obeys the following model

$$y_j(t) = \sum_{i=1}^{Q} h_{ij}(t) \sqrt{\lambda(i,t)} \theta_i(t) I_i + n_j(t), \quad t = 1, 2, \ldots, T, \tag{20}$$

where $h_{ij}(t)$ are known weights corresponding to the beam pattern, $\lambda(i,t)$ is the energy allocated for measuring cell i, $\theta_i(t)$ is a random return from cell i, and $n_j(t)$ is an additive observation noise, all at time t. Note that since the indicator of the ROI I_i is independent of t, this model

[6]Throughout this paper we refer to a search effort distribution as an effort allocation policy or just a search policy for brevity.

corresponds to a static scenario. We assume that the additive noise $n_j(t)$ is independent for varying j and t. Also, $\theta_i(t) > 0$ follows a prior distribution $p_\Theta(\theta)$ and is independent for different i but may be dependent for different t. The model in (20) can be written as

$$\boldsymbol{y}(t) = H(t)'\text{diag}\{\sqrt{\boldsymbol{\lambda}(t)}\}\text{diag}\{\boldsymbol{\theta}(t)\}\boldsymbol{I}_\Psi + \boldsymbol{n}(t), \tag{21}$$

where $\boldsymbol{y}(t) = [y_1(t), y_2(t), \ldots, y_{M_t}(t)]'$, $[H(t)]_{ij} = h(t)_{ij}$, $\boldsymbol{\lambda}(t) = [\lambda(1,t), \lambda(2,t), \ldots, \lambda(Q,t)]'$, $\boldsymbol{\theta}(t) = [\theta_1(t), \theta_2(t), \ldots, \theta_Q(t)]'$, $\boldsymbol{I}_\Psi = [I_1, I_2, \ldots, I_Q]'$, and $\boldsymbol{n}(t) = [n_1(t), n_2(t), \ldots, n_{M_t}(t)]'$. The notation $\sqrt{\boldsymbol{\lambda}(t)}$ denotes an $Q \times 1$ vector with $[\sqrt{\boldsymbol{\lambda}(t)}]_i = \sqrt{\lambda(i,t)}$, while the operator $\text{diag}\{\boldsymbol{x}\}$ corresponds to an $Q \times Q$ (square) diagonal matrix with $x(i)$ as its ii^{th} element. Our interest is in a resource allocation scheme that improves the 'quality' of the measurements over the ROI, with respect to (w.r.t.) a uniform allocation. In addition we assume an energy constraint

$$\frac{1}{\lambda_T}\sum_{i=1}^{Q}\sum_{t=1}^{T}\lambda(i,t) = 1, \tag{22}$$

i.e., there is some total energy λ_T available for our disposal.

An important aspect to this problem is that at the time t, the energy allocated to cell i may depend on past observations, i.e., $\lambda(i,t)$ is a function of $\boldsymbol{y}(1), \boldsymbol{y}(2), \ldots, \boldsymbol{y}(t-1)$. In other words, we utilize information from past observation in our resource allocation scheme. While $\lambda(i,t)$ is used for brevity the full notation is $\lambda(i,t;\boldsymbol{y}(1),\boldsymbol{y}(2),\ldots,\boldsymbol{y}(t-1))$. Following (3), define Λ the cumulative energy distributed to cell i as $\Lambda(i) = \sum_{t=1}^{T}\lambda(i,t)$. Our cost function is $J(\Lambda)$, as defined in (5), and our goal is to minimize the expected cost in the r.h.s. of (19) over all possible energy allocations $\lambda(i,t)$, subject to (22). Consider $\nu = 1$ and let $p = \Pr(I_i = 1)$ be a uniform prior distribution on the location of targets. Note that p represent the sparsity of the vector $\boldsymbol{I}_\Psi$, i.e. $|\Psi|$ is a Binomial r.v. with $\mathrm{E}\{|\Psi|\} = pQ$. Define $p^* = \frac{|\Psi|}{Q}$ then $\mathrm{E}\{p^*\} = p$ and $\text{var}(p^*) = \frac{p(1-p)}{Q}$. Next,

$$J(\Lambda_o) \leqslant J(\Lambda) \tag{23}$$

for all Λ provides

$$G(\Lambda) \leqslant G(\Lambda_o) = -10\log p^*. \tag{24}$$

In Appendix IV we use (24) and Bernstein's inequality to prove that

$$\Pr(G(\Lambda) \leqslant -10\log p + \epsilon) \geqslant 1 - \delta \tag{25}$$

for some $\delta \geqslant \exp\{-Q\frac{3}{8}\frac{p}{1-p}\}$ and $\epsilon(\delta, p, Q)$. For example, using the numbers from the SAR imaging example in Section V we obtain

$$\Pr(G(\Lambda) \leqslant 20 + 0.333) \geqslant 0.999.$$

III. SEARCH POLICY

In the following section, we solve the optimization problem previously defined, for $T = 2$, i.e., find

$$\hat{\lambda}(i,t) = \arg\min_{\lambda(i,t)} \mathrm{E}\left\{\sum_{i=1}^{Q} \frac{\nu I_i + (1-\nu)(1-I_i)}{\sum_{t=1}^{2}\lambda(i,t)}\right\}, \tag{26}$$

subject to the energy constraint $\frac{1}{\lambda_T}\sum_i\sum_t \lambda(i,t) = 1$. We assume a uniform prior to reflect no prior knowledge on the whereabouts of targets, and set $p_i = p$ for all i. The idea is to spend some energy to learn about the data domain and obtain a posterior distribution, then use the rest of the energy to search an estimate of the ROI. Define the auxiliary variable $\lambda^{(t)}$ as the total energy spent at search step t with $\frac{1}{\lambda_T}\sum_t \lambda^{(t)} = 1$, our goal is to optimize the energy distribution between steps and among cells in each step.

A. Optimal search policy

With $T = 1$ and a uniform prior, the minimizer of the cost in (26) is a uniform energy allocation (see appendix V-A for details), i.e.,

$$\lambda(i,1) = \frac{\lambda^{(1)}}{Q} \triangleq \lambda_1. \tag{27}$$

For $T = 2$ we need to optimize over the energy allocation between steps and within each step for the two steps together. In the rest of this section we restrict our discussion and consider only two step energy allocation schemes in which $\lambda(i,1) = C$, i.e., a uniform energy allocation at the first step. Therefore, we set

$$\lambda(i,1) = \lambda_1, \quad \forall i. \tag{28}$$

Since, $\lambda_T = Q\lambda_1 + \lambda^{(2)}$ optimizing the total effort allocated for each step is equivalent to finding an optimal pair $(Q\lambda_1, \lambda_T - Q\lambda_1)$, which is a single variable optimization task. Hence, our cost function simplifies to

$$J(\Lambda) = \sum_{i=1}^{Q} \mathrm{E}\left\{\frac{\nu I_i + (1-\nu)(1-I_i)}{\lambda_1 + \lambda(i,2)}\right\}, \tag{29}$$

where expectation is taken w.r.t. $\boldsymbol{y}(1)$ and $\boldsymbol{I}_\Psi$. Note that $\lambda(i,2)$ depends only on $\boldsymbol{y}(1)$, thus $\boldsymbol{y}(2)$ does not affect the cost function and can be omitted from the expectation. In addition, (29) is constant in $\boldsymbol{\theta}$ and therefore we omit it from the expectation as well. Next, we optimize over the effort distribution between the two steps and within the second step. Rewriting (29) using iterated expectation yields

$$J(\Lambda) = \sum_{i=1}^{Q} \mathrm{E}\left\{ \mathrm{E}\left\{ \frac{\nu I_i + (1-\nu)(1-I_i)}{\lambda_1 + \lambda(i,2)} \middle| \boldsymbol{y}(1) \right\} \right\}. \tag{30}$$

Note that I_i is binary random variable (r.v.). In addition, given $\boldsymbol{y}(1)$, $\lambda(i,2)$ is deterministic. Hence (30) becomes

$$\sum_{i=1}^{Q} \mathrm{E}\left\{ \frac{\mathrm{E}\left\{\nu I_i + (1-\nu)(1-I_i)|\boldsymbol{y}(1)\right\}}{\lambda_1 + \lambda(i,2)} \right\} = \tag{31}$$

$$\sum_{i=1}^{Q} \mathrm{E}\left\{ \frac{\nu \mathrm{Pr}\left(I_i = 1|\boldsymbol{y}(1)\right) + (1-\nu)(1-\mathrm{Pr}\left(I_i = 1|\boldsymbol{y}(1)\right))}{\lambda_1 + \lambda(i,2)} \right\}. \tag{32}$$

Using Bayes rule for the numerator, we have

$$\mathrm{Pr}(I_i = 1|\boldsymbol{y}(1)) = \frac{P(\boldsymbol{y}(1)|I_i = 1)p}{P(\boldsymbol{y}(1)|I_i = 1)p + P(\boldsymbol{y}(1)|I_i = 0)(1-p)} \stackrel{\triangle}{=} p_{I_i|\boldsymbol{y}(1)}, \tag{33}$$

where

$$P(\boldsymbol{y}|I_i) = \int P(\boldsymbol{y}|I_i, \theta_i) p_\Theta(\theta) d\theta \tag{34}$$

is the given conditional probability model describing the measurement dependency on the presence of targets. Finally, we can rewrite our cost function (26), and solve the following

$$\hat{\lambda}(i,t) = \arg \min_{\lambda_1, \lambda(i,2)} \mathrm{E}\left\{ \sum_{i=1}^{Q} \frac{\nu p_{I_i|\boldsymbol{y}(1)} + (1-\nu)(1-p_{I_i|\boldsymbol{y}(1)})}{\lambda_1 + \lambda(i,2)} \right\}, \tag{35}$$

where expectation is taken w.r.t. $\boldsymbol{y}(1)$. For a given $p_\Theta(\theta)$ and a general prior distribution we derive an optimal solution for $\lambda(i,2)$ in appendix V. The special case of interest where the prior distribution is uniform, i.e., $\lambda(i,1) = \lambda_1$ is given below. Let λ_1 be the energy allocated to each cell at the first step, with $Q\lambda_1 = \lambda^{(1)} \leqslant \lambda_T$. Define $W_j = \nu p_{I_j|\boldsymbol{Y}} + (1-\nu)(1-p_{I_j|\boldsymbol{Y}})$ with a corresponding random realization $\boldsymbol{w} = [w_1, w_2, \ldots, w_Q]'$. Let $\tau : \mathcal{X} \to \mathcal{X}$ be a permutation operator defined as

$$\tau(j) = \arg \min_{i=1,\ldots,Q} \{w_i : w_i \geqslant w_{\tau(j-1)}\}, \qquad j \in \{1, 2, \ldots, Q\}, \tag{36}$$

with $w_{\tau(0)} \equiv 0$. Whenever the r.h.s. of (36) is not unique we pick an arbitrary i satisfying $w_{\tau(1)} \leqslant w_{\tau(2)} \leqslant \ldots \leqslant w_{\tau(Q)}$.

Assuming $w_{\tau(1)} > 0$, define $k_0 = 0$ if

$$\frac{\lambda_T}{\lambda_1} > \frac{\sum_{i=1}^{Q} \sqrt{w_{\tau(i)}}}{\sqrt{w_{\tau(1)}}}, \tag{37}$$

otherwise $k_0 \in \{1, \ldots, Q-1\}$ is the unique solution, satisfying

$$\frac{\sum_{i=k_0+1}^{Q} \sqrt{w_{\tau(i)}}}{\sqrt{w_{\tau(k_0+1)}}} < \frac{\lambda_T}{\lambda_1} - k_0 \leqslant \frac{\sum_{i=k_0+1}^{Q} \sqrt{w_{\tau(i)}}}{\sqrt{w_{\tau(k_0)}}}. \tag{38}$$

Given λ_1 and k_0, we show in Appendix V that the optimal energy allocation $\lambda(\tau(i), 2)$, minimizing our cost, is

$$\lambda(\tau(i), 2) = \left(\frac{\lambda_T - k_0 \lambda_1}{\sum_{j=k_0+1}^{Q} \sqrt{w_{\tau(j)}}} \sqrt{w_{\tau(i)}} - \lambda_1 \right) I(i > k_0). \tag{39}$$

Therefore, the optimization problem has translate to; find λ_1^* minimizing

$$\lambda_1^* = \arg\min_{\lambda_1} \mathrm{E} \left\{ \sum_{i=1}^{Q} \frac{W_{\tau(i)}}{\lambda_1 + \left(\frac{\lambda_T - k_0 \lambda_1}{\sum_{j=k_0+1}^{Q} \sqrt{W_{\tau(j)}}} \sqrt{W_{\tau(i)}} - \lambda_1 \right) I(i > k_0)} \right\} = \tag{40}$$

$$\arg\min_{\lambda_1} \mathrm{E} \left\{ \frac{1}{\lambda_1} \sum_{i=1}^{k_0} W_{\tau(i)} + \frac{1}{\lambda_T - k_0 \lambda_1} \sum_{i=k_0+1}^{Q} \sum_{j=k_0+1}^{Q} \sqrt{W_{\tau(i)} W_{\tau(j)}} \right\}, \tag{41}$$

where if $k_0 = 0$ then the first summation in (41) equals zero. We can find λ_1^* via a grid search. In summary, define the optimal policy minimizing (35) as follows

Algorithm 1: Adaptive Resource Allocation Policy (ARAP)

Step 1: Allocate λ_1^* to each cell.

Step 2: Given $\boldsymbol{y}(1)$ derive w_i via $P_{I_i|y_i(1)}$ defined in (33).

Step 3: Sort the w_i's then use λ_1^* and the ordered statistic $w_{\tau(i)}$ to derive k_0 using (37) and (38).

Step 4: Given k_0, define $\lambda(i, 2)$ the allocated energy to cell i as

$$\lambda(\tau(i), 2) = \left(\frac{\lambda_T - k_0 \lambda_1^*}{\sum_{j=k_0+1}^{Q} \sqrt{w_{\tau(j)}}} \sqrt{w_{\tau(i)}} - \lambda_1^* \right) I(i > k_0). \tag{42}$$

Let λ_A denote a search policy due to *ARAP*, then $\lambda_A(i, 1) = \lambda_1^*$ and $\lambda_A(i, 2)$ is given in (42). Note that *ARAP* follows the same logic as the well known water-filling algorithm [30] (pp.

277). Water-filling is the solution for an optimal power distribution among parallel Gaussian communication channels, maximizing the over all capacity subject to a total power constraint. If each channel has variance N_i and allotted power P_i, Water-filling maximizes $\sum_i \frac{1}{2}\log(1+\frac{P_i}{N_i})$ subject to $\sum_i P_i = P$. Both *ARAP* and Water-filling calculate a certain threshold and distribute efforts only where it serve to reduce or increase the cost function respectively.

B. Properties of the optimal energy allocation

Theorem 1: For some $\nu \in [\frac{1}{2}, 1]$ and λ_1^*, let $\Lambda_A(i)$ be an effort allocation distribution, due to *ARAP*. Then, for a uniform prior distribution, we have

$$J(\Lambda_A) \leqslant J(\Lambda_U), \tag{43}$$

with equality achieved if $P_{I_i|\boldsymbol{y}(1)} = c,\ \forall i$.

Proof: Note that a uniform effort allocation scheme can be broken into any arbitrarily number, T, of consecutive search steps, as long as for all i

$$\Lambda_U(i) = \sum_{t=1}^{T} \lambda(i,t) = \frac{\lambda_T}{Q}. \tag{44}$$

Without loss of generality (wlog) let $T = 2$, let P denotes the family of all effort allocation policies λ defined as

$$P = \left\{ \lambda(i,t) : \sum_{i=1}^{Q}\sum_{t=1}^{2} \lambda(i,t) = \lambda_T,\ \lambda(i,1) = \lambda_1 \geqslant 0,\ \lambda(i,2) \geqslant 0 \right\}, \tag{45}$$

and note that $\exists \lambda \in P$ satisfying (44). Also note that *ARAP* yields Λ_A optimal over all $\lambda \in P$. Hence, Λ_U is just a special solution that *ARAP* may assume. Since *ARAP* yields the optimal effort allocation for any posterior distributions $\{P_{I_i|\boldsymbol{y}(1)}\}_{i=1}^{Q}$, we have $J(\Lambda_A) \leqslant J(\Lambda_U)$. To show the equality part note that if $P_{I_i|\boldsymbol{y}(1)} = c$ for all i, then $w_i = c',\ \forall i$, for which *ARAP* yields $k_0 = 0$. Furthermore, from (42) we get

$$\lambda_A(i,2) = \frac{\lambda_T}{Q} - \lambda_1, \tag{46}$$

or, equivalently, $\Lambda_A(i) = \frac{\lambda_T}{Q} = \Lambda_U(i)$. Therefore, the two sides of (43) are equal. This completes the proof. ■

ARAP is optimal over all policies that allocates energy uniformly at the first step. With a uniform prior, allocating energy uniformly at the first step provides the most informative posterior distribution $p(\boldsymbol{I}_\Psi|\boldsymbol{y})$ on the average. Note that in Appendix V we solve for the general case of a non uniform prior. However, in the general case $\lambda^*(i,1)$ depends on the specific prior and is a function of i. Therefore, the optimization problem is far more complex and in general not tractable.

Note that *ARAP* uses k_0 to concentrate effort allocation onto an estimated ROI. Define

$$\widehat{\Psi} = \{i : \lambda_A(i,2) > 0\}, \tag{47}$$

then $\Lambda(i) > \Lambda(j)$ for all $i \in \widehat{\Psi}$ and $j \in \widehat{\Psi}^c$. We interpret this part as an intermittent detection/classification process. This is not equivalent to estimating the ROI based on the measurement pair $(\boldsymbol{y}(1), \boldsymbol{y}(2))$, which is presented in Section IV-C.

1) Asymptotic properties of the optimal solution: Next we analyze some asymptotic properties of the optimal solution (42), when $\nu = 1$. By asymptotic conditions we mean high SNR[7] for the exhaustive search policy and large Q. For *ARAP*, we show:

$$\mathrm{E}\{k_0\} \to (1-p)Q, \tag{48}$$

$$\lambda_1^* \to 0, \tag{49}$$

$$G(\Lambda_A) \to -10 \log p. \tag{50}$$

Note that $p_{I_i|\boldsymbol{y}(1)}$ defined in (33) is the conditional mean estimator of I_i. We prove the asymptotic properties described above assuming that

$$p_{I_i|\boldsymbol{y}(1)} \to I_i, \tag{51}$$

for high SNR, in either probability or in the mean squared error. This can be easily shown (see Appendix VI) for the Gaussian case, where $y_i(1) \sim \mathcal{N}(\sqrt{\lambda_1}\theta_i I_i, \sigma^2)$, and we speculate that (51) holds for other cases as well. Hence, for high SNR, the set $\{p_{I_i|y_i}\}_{i=1}^Q$ can be approximated as,

[7]From hereon, we use the term SNR to denote the signal to noise ratio per cell, that an exhaustive search policy with equal energy allocation scheme would exhibit, i.e., SNR=$\frac{\lambda_T/Q}{\sigma^2}$.

i.i.d., Bernoulli r.v.'s, with $\Pr(p_{I_i|y_i}=1)=p$. Therefore, for any realization, $\exists\tilde{k}$ such that the ordered posterior probabilities obey

$$p_{I_{\tau(i)}|y_{\tau(i)}}=\begin{cases}0, & i\leqslant\tilde{k}\\ 1, & i>\tilde{k}\end{cases}. \tag{52}$$

Evaluating inequalities (38) for $k_0=\tilde{k}$, yields

$$Q<\frac{\lambda_T}{\lambda_1}\leqslant\infty. \tag{53}$$

Hence, $\forall\lambda_1>0$, the desired solution of (38) is $k_0=\tilde{k}$. Moreover, $\tilde{k}=Q-\sum_i I(p_{I_i|y_i}=1)$ equals the total number of zeros in the sequence, and is a Binomial random variable distributed $\tilde{k}\sim B(Q,1-p)$, thus

$$\mathrm{E}\{k_0\}=(1-p)Q. \tag{54}$$

Substituting $\tilde{k}$ for k_0 and using the fact that $w_{\tau(i)}=p_{I_{\tau(i)}|y_{\tau(i)}}=0$ for $\tau(i)\leqslant\tilde{k}$ in (41) yields

$$\lambda_1^*=\arg\min_{\lambda_1}\mathrm{E}\left\{\frac{(Q-\tilde{k})^2}{\lambda_T-\tilde{k}\lambda_1}\right\}, \tag{55}$$

and since $\tilde{k}\in\{1,2,\ldots,Q-1\}$, $\frac{(Q-\tilde{k})^2}{\lambda_T-\tilde{k}\lambda_1}$ is monotonically increasing in λ_1, regardless of the expectation operator. Thus, the minimizer w.r.t. λ_1 is achieved at the lowest possible value for λ_1. Since $\lambda_1\in(0,\frac{\lambda_T}{Q})$, the best one can do is to allocate the minimum feasible positive energy value to all cells at the first step. For large Q, this leads our optimal search policy to approach the lower bound for the cost function. Recall from (12) that the best possible search policy uniformly allocate the total among all cells in the ROI. Hence the expected minimal cost is $\mathrm{E}\{\frac{|\Psi|^2}{\lambda_T}\}=\frac{p^2Q^2+p(1-p)Q}{\lambda_T}$, letting $\lambda_1\to 0$ in our cost function yields

$$\lim_{SNR\to\infty}\mathrm{E}\left\{\frac{(Q-\tilde{k})^2}{\lambda_T-\tilde{k}\lambda_1}\right\}\cong\frac{\mathrm{E}\{(Q-\tilde{k})^2\}}{\lambda_T}=\frac{p^2Q^2+p(1-p)Q}{\lambda_T}, \tag{56}$$

therefore, $G(\Lambda_A)\to-10\log p$. Figure 1 in section IV shows $G(\Lambda_A)$ for SNR values ranging from 0 to 40 [dB]. The three curve pairs corresponds to p values of $\frac{1}{1000}$, $\frac{1}{100}$, and $\frac{1}{10}$, with asymptotic gain values of 30, 20, and 10 [dB] respectively. Both our methods, the optimal and suboptimal (described below), are shown to converge to the theoretical limit.

For $\nu\in(\frac{1}{2},1)$, at high SNR, $w_{\tau(i)}$ converges to a discrete r.v. W, with $\Pr(W=\nu)=p$ and $\Pr(W=1-\nu)=1-p$. As before, $\exists\tilde{k}$ such that $w_{\tau(i)}=1-\nu$ for all $\tau(i)\leqslant\tilde{k}$, and

$w_{\tau(i)} = \nu,\ \forall \tau(i) > \tilde{k}$. Evaluating inequalities (38), for this case yield one of two solutions:

$$\frac{\lambda_T}{\lambda_1} > \tilde{k} + (Q - \tilde{k})\sqrt{\frac{\nu}{1-\nu}} \quad \Rightarrow \quad k_0 = 0, \tag{57}$$

$$\frac{\lambda_T}{\lambda_1} \leqslant \tilde{k} + (Q - \tilde{k})\sqrt{\frac{\nu}{1-\nu}} \quad \Rightarrow \quad k_0 = \tilde{k}. \tag{58}$$

Note that as $\nu \to 1$ the r.h.s. of the inequalities in (57)-(58) approaches infinity, thus we have convergence to the result previously shown.

C. Suboptimal search policy

Next, as a simple alternative to *ARAP*, we consider a search policy where $\lambda(i,1) = C$ and

$$\lambda(i,2) = \frac{\lambda_T - QC}{\sum_{j=1}^{Q}\sqrt{w_j}}\sqrt{w_i},$$

leading to a corresponding cumulative energy allocation Λ. Substituting Λ in (35) yields a single variable optimization problem and we grid search C to find C^* minimizing the expected cost. Finally we define $\lambda_{so}(i,1) = C^*$ and

$$\lambda_{so}(i,2) = \frac{\lambda_T - QC^*}{\sum_{j=1}^{Q}\sqrt{w_j}}\sqrt{w_i}, \tag{59}$$

with its equivalent cumulative energy allocation Λ_{so}. On top of being simple, (59) is optimal for two extreme cases: (i) uniform posterior distribution, (ii) high SNR posterior distribution with L elements for which $p_{I_i|\boldsymbol{y}(1)} = 1$ and $(Q-L)$ elements for which $p_{I_i|\boldsymbol{y}(1)} = 0$, when $\nu = 1$. For (i) we get a uniform energy allocation, while for (ii), (59) results in

$$\lambda_{so}(i,2) = \begin{cases} \frac{\lambda_T - Q\lambda_1}{L}, & p_{I_i|\boldsymbol{y}(1)} = 1 \\ 0, & \text{Otherwise} \end{cases}, \tag{60}$$

both equivalent to the optimal mapping (42). Although (59) does not make the analytical evaluation of the expectation in (29) tractable, it is less computational demanding than the optimal solution. Both λ_A and λ_{so} has complexity level of $\mathcal{O}(Q)$, albeit there is an $\mathcal{O}(\log Q)$ difference in their complexity levels. This stems from the fact that *ARAP* requires both sorting of the w_i's and finding the threshold k_0. Therefore, performance comparison between the two is interesting since it shows what we loose by the much simpler suboptimal solution. In section IV we compare the two policies and show that λ_{so} is nearly optimal in terms of our cost function. Moreover, it turns out that considering a detection problem as a post processing task the suboptimal solution is equivalent or better than the more computational demanding optimal solution.

D. A note on multi-step search

An outline for the optimal solution in the case where $T > 2$ is given in appendix V-C. We show how to simplify the problem from optimizing the energy allocated to each cell to optimizing the over all energy allocated per search step. Define $\lambda^{(t)}$ the total energy used in step t, where $\lambda^{(t)} = \sum_{i=1}^{Q} \lambda(i,t)$ and $\lambda_T = \sum_{t=1}^{T} \lambda^{(t)}$. An optimal solution for the last step, $\{\lambda(i,t)\}_{i=1}^{Q}$, is provided but a global optimum requires solving a backward induction optimizing over $\{\lambda^{(1)}, \ldots, \lambda^{(T-1)}\}$. Unfortunately, the problem becomes numerically intractable as T increases. Nevertheless, for any step t, we may use the general version of *ARAP*, proposed in (136) in Appendix V, as a "two step lookahead" optimal search policy. Appendices V-A and V-B provide a solution for a general prior distribution. Hence, at any step t we may treat the latest posterior distribution, obtained by steps $\{1, 2, \ldots, t-1\}$, as the new prior distribution and solve a two step energy allocation problem. Once we find the optimal two-step energy allocation, we use the solution given in appendix V-A for step t while the rest of the energy is kept for search steps $\{t+1, \ldots, T\}$.

IV. Comparison of search algorithms

Assume either λ_A or λ_{so} were used to generate data vectors $(\boldsymbol{y}(1), \boldsymbol{y}(2))$. A natural question is whether or not this data is better in some sense than the measurement vector $\boldsymbol{y}$ obtained using the standard exhaustive search policy. In this section, we compare performance of both the optimal effort allocation policy and the suboptimal solution to those achieved by an exhaustive search scheme for different tasks. We start by comparing the averaged cost achieved by λ_A and λ_{so}, and proceed by comparing two post-processing tasks estimation and detection, based on data measured using each policy. In the following section we assumed $\theta_i(t) = \theta_i$ is an independent and identically distributed (i.i.d.) truncated Gaussian random variables with mean $\mu_\theta = 1$ and standard deviation $\sigma_\theta = 0.25$, for all i.

A. Achievable cost

First we compare the average performance gain $G(\cdot)$, defined in (17), achieved by the two search policies for $\nu = 1$. We chose $Q = 8192$ as the total number of cells and the sparsity values of $p \in \{\frac{1}{10}, \frac{1}{100}, \frac{1}{1000}\}$, i.e., a mean of roughly 800, 80, and 8 targets per realization, respectively. Results are shown in Figures 1(a) and 1(b) where the curves with crosses describe the gain from the optimal allocation *ARAP* $G(\Lambda_A)$ and curves with circles describe the gain

from the suboptimal allocation $G(\Lambda_{so})$, for all three p values. Figure 1(a) shows the behavior of the gain for the two policies for SNR values of 0[dB] to 40[dB]. Figure 1(b) zooms in on SNR values of 0[dB] to 13[dB]. Each point on a graph represents 500 runs in a Monte Carlo simulation. As can be seen from Fig. 1(a), at extreme high or low SNR values the performance gain of the two policies is equal. We use Fig. 1(a) to establish that the gain converges to its theoretical limit given by (50). The largest gap in gain between the two algorithms is at the transition zone: SNR between 5-15 [dB], and the gap is less than 2 [dB]. Evidently, the simpler suboptimal mapping rule does not significantly degrade performance gain.

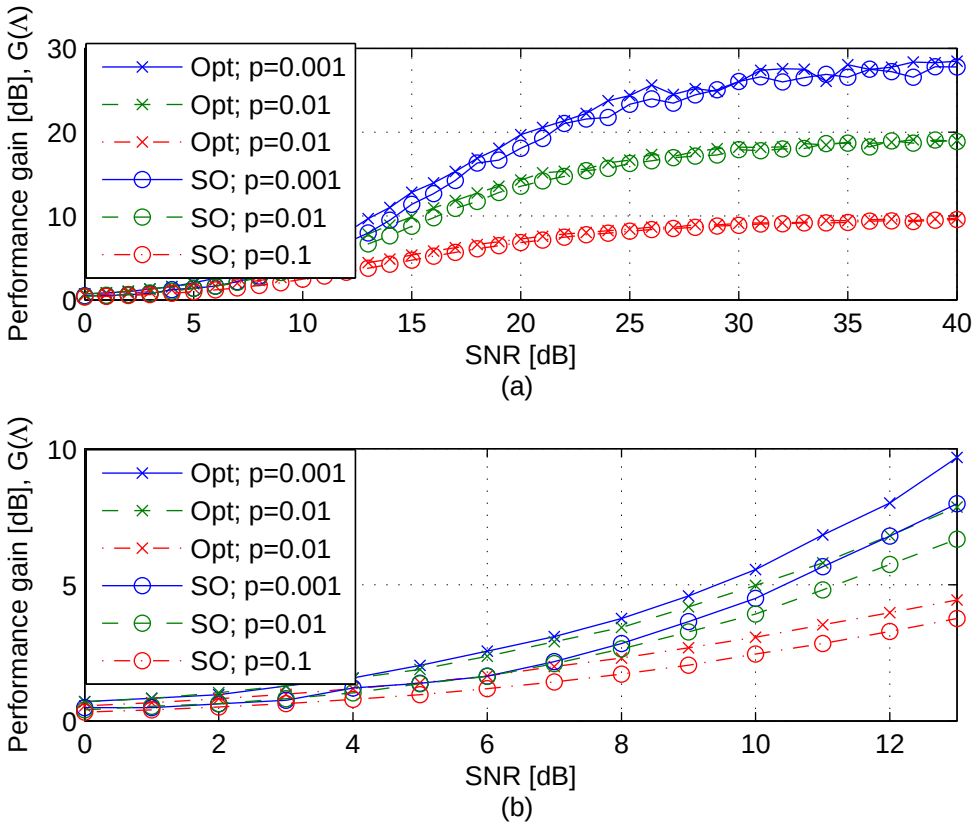

Fig. 1. We display the cost gain compared to an exhaustive search for both our optimal and suboptimal energy allocation schemes. (a) shows that both algorithms converges to the asymptotic predicted gain, at $-10\log p$. (b) enhances the difference between our two policies for SNR values in the range of $0-13$ [dB].

Figure 2 compares the percentage of effort $\frac{\lambda^{(1)}}{\lambda_T}$ allocated in the first step for both policies. While for SNR values greater than 25 [dB] the curves overlap, this is not the case for low SNR values. As measurement quality decreases, *ARAP* invests more energy at the first step.

Considering the difference between the two policies, this result makes sense: after the first step *ARAP* ignores all cells with posterior probability values lower than some threshold. Wrong decision at that stage can no longer be compensated, i.e., the cumulative effort distribution $\Lambda_\lambda(i)$ for those cells will remain unchanged. Hence, more effort has to be allocated to the first step so that decisions would be made to improve the agreement between $\widehat{\Psi}$ and Ψ. On the other hand, the suboptimal mapping invests energy in all Q cells at the second step. Thus, it has a chance to compensate for poor estimated posterior probability values.

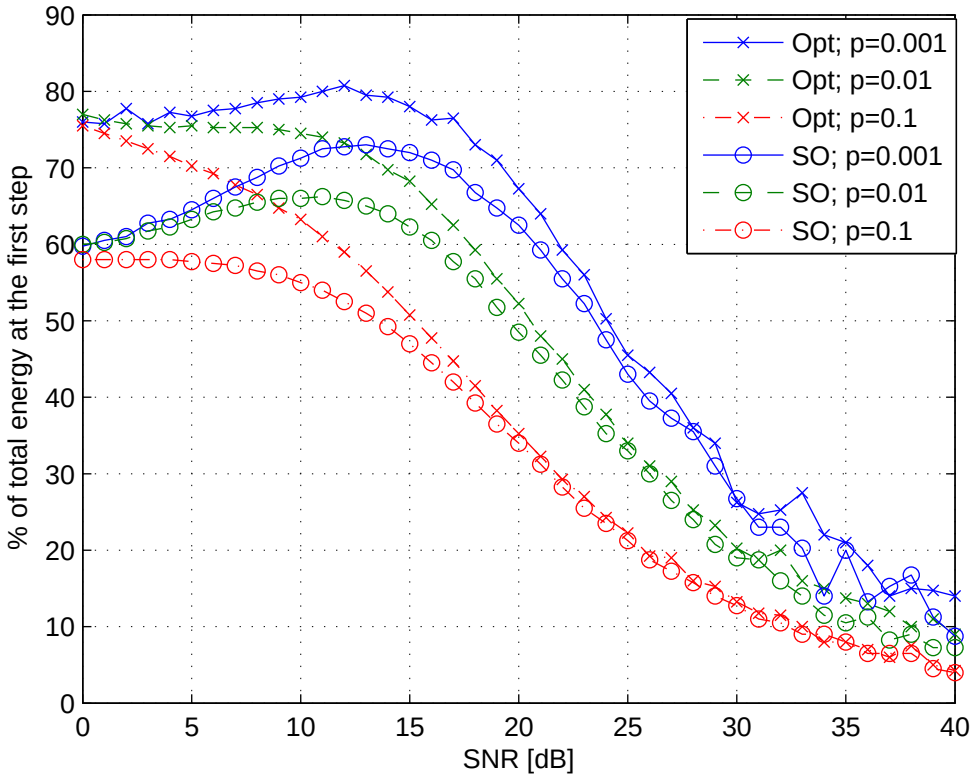

Fig. 2. We compare the proportion of energy invested at the first step for the two algorithms λ_A and λ_{so}. Curves correspond to prior probability values of $0.001, 0.01$ and 0.1. As seen, the optimal search policy invest more energy at the first step. However, for SNR > 25[dB] the two are essentially equivalent.

B. Post-processing estimation task

Consider the problem of estimating the true value of each target return θ_i in (20). For estimation the choice of $\nu = 1$ seems natural. Recall that in Section II we claimed that minimizing our cost

is entirely equivalent, in the Gaussian case, to minimizing the estimation mean squared error (MSE). Assuming $\theta_i \sim \mathcal{N}(\mu_\theta, \sigma_\theta^2)$ we use a Bayesian framework for estimating θ_i based on its prior distribution. The optimal estimator minimizing the MSE is the conditional mean estimator (CME). We compare the performance of $\mathrm{E}\{\theta|\boldsymbol{y}\}$ the CME for an exhaustive search policy to $\mathrm{E}\{\theta|\boldsymbol{y}(1), y_i(2)\}$ a CME for either *ARAP* or the suboptimal search policy. The MSE of the CME for the exhaustive search policy is given by

$$\mathrm{var}\{\theta_i|y_i\} = \sigma_\theta^2 - \frac{\varepsilon_0\sigma_\theta^4}{\sigma^2 + \varepsilon_0\sigma_\theta^2} = \frac{\sigma_\theta^2}{1 + \varepsilon_0\frac{\sigma_\theta^2}{\sigma^2}}. \tag{61}$$

The competing estimator is a Naive Bayes estimator of $\mathrm{E}\{\theta|\boldsymbol{y}(1), y_i(2)\}$, which assumes that $(\boldsymbol{y}(1), y_i(2))$ are independent [31], defined as

$$\hat{\theta}_i = \mu_\theta + \frac{y_i(1)\sqrt{\lambda_1} + y_i(2)\sqrt{\lambda(i,2)} - \mu_\theta(\lambda_1 + \lambda(i,2))}{\lambda_1 + \lambda(i,2) + \sigma^2/\sigma_\theta^2}. \tag{62}$$

Monte-Carlo simulations were used to estimate the MSE of (62). In Fig. 3, we plot the performance gain, defined as $10\log\frac{\mathrm{var}(\theta_i|y_i)}{\mathrm{MSE}(\hat{\theta}_i)}$ as a function of SNR. We chose $Q = 4096$, $p \in \{\frac{1}{10}, \frac{1}{100}\}$, and each point on the figure represents an average over θ based on 2000 realizations. Note that the MSE performance gain follows the performance gain for the cost function (5), as seen on Figure 1. In addition *ARAP* yield better estimation performance compared to the suboptimal policy. This reinforces the connection between our cost function (5) and estimation MSE.

C. Post-processing detection task

Consider the problem of correctly detecting whether cell i contains a target. As before, we assume an i.i.d. additive white Gaussian noise in (20) and $\theta_i \sim \mathcal{N}(\mu_\theta, \sigma_\theta^2)$. Thus, for an exhaustive search policy $y_i \sim \mathcal{N}(\sqrt{\lambda_0}\mu_\theta I_i, \sigma_y^2)$, where $\sigma_y^2 = \sigma^2 + \lambda_0\sigma_\theta^2$. Given y_i the measurement of pixel i, our goal is to decide between

$$\begin{aligned} H_0 &: y_i \sim \mathcal{N}(0, \sigma_y^2), \\ H_1 &: y_i \sim \mathcal{N}(\sqrt{\lambda_0}\mu_\theta, \sigma_y^2). \end{aligned} \tag{63}$$

The uniformly most powerful test for this simple binary hypothesis testing problem is a likelihood ratio test (LRT). The performance of the LRT in terms of its receiver operating characteristic

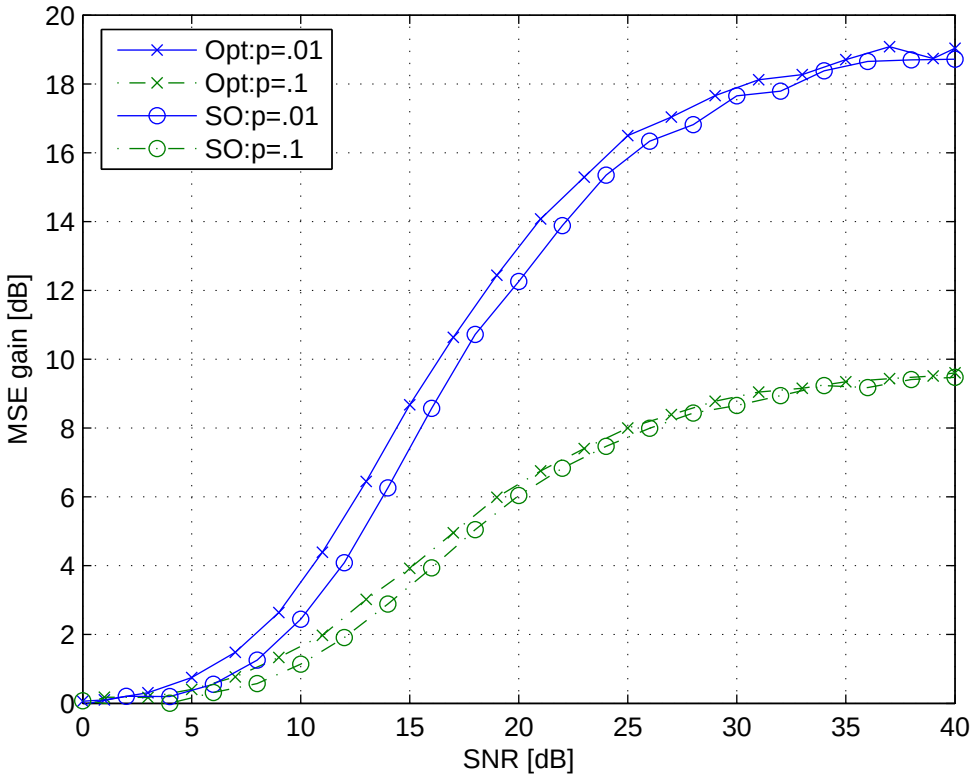

Fig. 3. Gain in MSE for the CME in (62) based on an adaptive search compared to the MSE of the CME for an exhaustive search policy (61). Curves with crosses correspond to *ARAP*, for p values of $\frac{1}{100}$ and $\frac{1}{10}$, while curves with circles represent the suboptimal adaptive policy. The MSE gain for *ARAP* is slightly higher than that of the suboptimal mapping. Note that using our methods results in about 6[dB] gain in MSE at SNR value of 12[dB] for sparsity level of 1%. In addition MSE gain is inversely proportional to the sparsity, hence higher gains can be expected for application where $|\Psi| \ll Q$.

(ROC) curve are easily calculated in this Gaussian case. The power β of a level α LRT is [32][8]

$$\beta = 1 - \Phi\left(\Phi^{-1}(1-\alpha) - \sqrt{\frac{\lambda_0 \mu_\theta^2}{\sigma^2 + \lambda_0 \sigma_\theta^2}}\right), \tag{64}$$

where $\Phi(\cdot)$ is the normal cumulative distribution function. In the following few lines we derive the likelihood function $f(\boldsymbol{y}(2), \boldsymbol{y}(1); \boldsymbol{I}_\Psi)$. Bayes rule provides

$$f(\boldsymbol{y}(2), \boldsymbol{y}(1)) = f(\boldsymbol{y}(2)|\boldsymbol{y}(1)) f(\boldsymbol{y}(1)), \tag{65}$$

[8]see pp. 69. Note that Kay defines $Q = 1 - \Phi$ and replace SNR=$\frac{NA^2}{\sigma^2}$ and $\alpha = P_{FA}$.

but given $\boldsymbol{y}(1)$ the measurements at the second step are independent for different cells and thus

$$f(\boldsymbol{y}(2),\boldsymbol{y}(1)) = \prod_{i=1}^{Q} f(y_i(2)|\boldsymbol{y}(1)) f(y_i(1)). \tag{66}$$

Therefore, the LRT statistics T_j is

$$T_j = \frac{\prod_{i=1}^{Q} f(y_i(2)|\boldsymbol{y}(1), I_j = 1) f(y_i(1)|I_j = 1)}{\prod_{i=1}^{Q} f(y_i(2)|\boldsymbol{y}(1), I_j = 0) f(y_i(1)|I_j = 0)} = \tag{67}$$

$$\frac{f(y_j(2)|\boldsymbol{y}(1), I_j = 1) f(y_j(1)|I_j = 1)}{f(y_j(2)|\boldsymbol{y}(1), I_j = 0) f(y_j(1)|I_j = 0)}. \tag{68}$$

For our model, we have $y_i(1) \sim \mathcal{N}(\sqrt{\lambda_1}\mu_\theta I_i, \sigma^2 + \lambda_1\sigma_\theta^2)$ and given $\boldsymbol{y}(1)$ the second step measurements $y_i(2) \sim \mathcal{N}(\sqrt{\lambda(i,2)}\mu_\theta I_i, \sigma^2 + \lambda(i,2)\sigma_\theta^2)$. Substituting those distributions in (68) provides the following LRT

$$\frac{\exp\left\{-\frac{1}{2(\sigma^2+\lambda(i,2)\sigma_\theta^2)}\left(y_i(2) - \mu_\theta\sqrt{\lambda(i,2)}\right)^2 - \frac{1}{2(\sigma^2+\lambda_1\sigma_\theta^2)}\left(y_i(1) - \mu_\theta\sqrt{\lambda_1}\right)^2\right\}}{\exp\left\{-\frac{y_i^2(1)}{2(\sigma^2+\lambda_1\sigma_\theta^2)} - \frac{y_i^2(2)}{2(\sigma^2+\lambda(i,2)\sigma_\theta^2)}\right\}} \gtrless \gamma,$$

which simplifies to

$$T_i = \mu_\theta\left(\frac{y_i(1)\sqrt{\lambda_1}}{\sigma^2+\lambda_1\sigma_\theta^2} + \frac{y_i(2)\sqrt{\lambda(i,2)}}{\sigma^2+\lambda(i,2)\sigma_\theta^2}\right) - \frac{\mu_\theta^2}{2}\left(\frac{\lambda_1}{\sigma^2+\lambda_1\sigma_\theta^2} + \frac{\lambda(i,2)}{\sigma^2+\lambda(i,2)\sigma_\theta^2}\right) \gtrless \gamma', \tag{69}$$

where $\gamma' = \log\gamma$. Note that for all cells where $\lambda(i,2) = 0$ this test is a function of $y_i(1)$ alone. As an alternative to (69), we also used the Benjamini-Hochberg procedure for controlling the false discovery rate (FDR) as a method for jointly detecting the structure of $\boldsymbol{I}_\Psi$. We used Monte-Carlo simulation of the test statistic T_i to compute its empiric cumulative distribution function and empiric p-values. The p-values were then processed according to the algorithm suggested in [33] to jointly detect elements in $\boldsymbol{I}_\Psi$ containing targets.

We compared the ROC curve (64) to an empiric ROC curve calculated for the test (69) performed on the data pair $(\boldsymbol{y}(1),\boldsymbol{y}(2))$ generated via both *ARAP* and the suboptimal mapping and to an empiric ROC curve of the FDR procedure using $(\boldsymbol{y}(1),\boldsymbol{y}(2))$ generated via *ARAP*. We conducted multiple runs for varying SNR levels and observed that with $\nu = 1$ (69) provides higher detection probability than (64) for test levels lower than roughly 30% for both our adaptive measurements scheme. At SNR values close to 0 [dB] the difference between the two tests is negligible, but the incentive to use our methods increases with SNR. Also, for very low false alarm levels *ARAP* performs better than the suboptimal mapping in terms of detection probability.

However, for higher test levels the suboptimal search policy yield better detection performances. In addition, using the Benjamini-Hochberg procedure to perform a joint detection test did not yield any performance gain.

Results are presented here for SNR=10 [dB], $Q = 1024$, and either $p = 0.1$ or $p = 0.01$. Monte-Carlo simulations were conducted with $\nu = 1$ and the results are shown in Figure 4 (a) and (b). Each point at the figures represents an average over 2000 realizations, and detection probability was averaged over the entire ensemble. At 10 [dB] the ROC curves are very sharp, hence plotted on a logarithmic scale. The solid curve represent a test based on an exhaustive with equal energy allocation (64). Curves with crosses represent the optimal policy, curves with circles represent the sub-optimal policy, and curves with triangles represent the FDR procedure. Figure 4(a) shows the entire ROC curves, it is evident that the different tests exhibits different slopes for low false alarm values. Moreover, for high false alarm values no adaptive policy outperforms the exhaustive search policy when $\nu = 1$. Figure 4(b) zooms in to enhance the difference between tests for $P_{fa} \in [0.008, 0.5]$. One can see that the optimal search policy has the best performances up to $\alpha = 3\%$, at which point the suboptimal policy yields higher detection probability. The exhaustive search policy outperforms both the adaptive methods for $\alpha > 30\%$. Our results suggest that performance of detector with false alarm less than 25% would be improved by the optimal and suboptimal search policies.

Since an exhaustive search policy is a special case of the adaptive search policy for $\nu = \frac{1}{2}$, we scanned all ν values to search for the best ν, maximizing P_D for a given P_{fa}. For every ν, we performed a grid search to find the optimal $\lambda_1^*(\nu)$ when substituting it to (42) then plugging everything back to (35). Next we generated an ROC curve for each pair $(\nu, \lambda_1^*(\nu))$ and selected ν_0, the maximizer of the detection probability for every given false alarm probability. The set of points $(P_D(\nu_0), P_{fa})$ represent an envelope of all the different ROC curves achievable by our adaptive sampling scheme and the text (69). Next, we treated (42) as a function of two free variables (ν, λ_1) and grid searched the domain $[.5, 1] \times (0, 1)$ for the best combination in terms of detection probability. Figures 5(a) and 5(b) compare the global detection optimum (dash-dotted curve with asterisks) with the envelope over ν (solid curve with crosses), to the ROC curve for $\nu = 1$ (dashed curve with plus markers) and to the exhaustive search ROC curve (solid) (64), as a function of the false alarm probability p_{fa}. Figure 5(a) has the full view, while 5(b) zooms in on an area of interest where $p_{fa} \in (0.07, .5)$. Figure 5(b) shows that $\nu = \frac{1}{2}$, i.e., an exhaustive

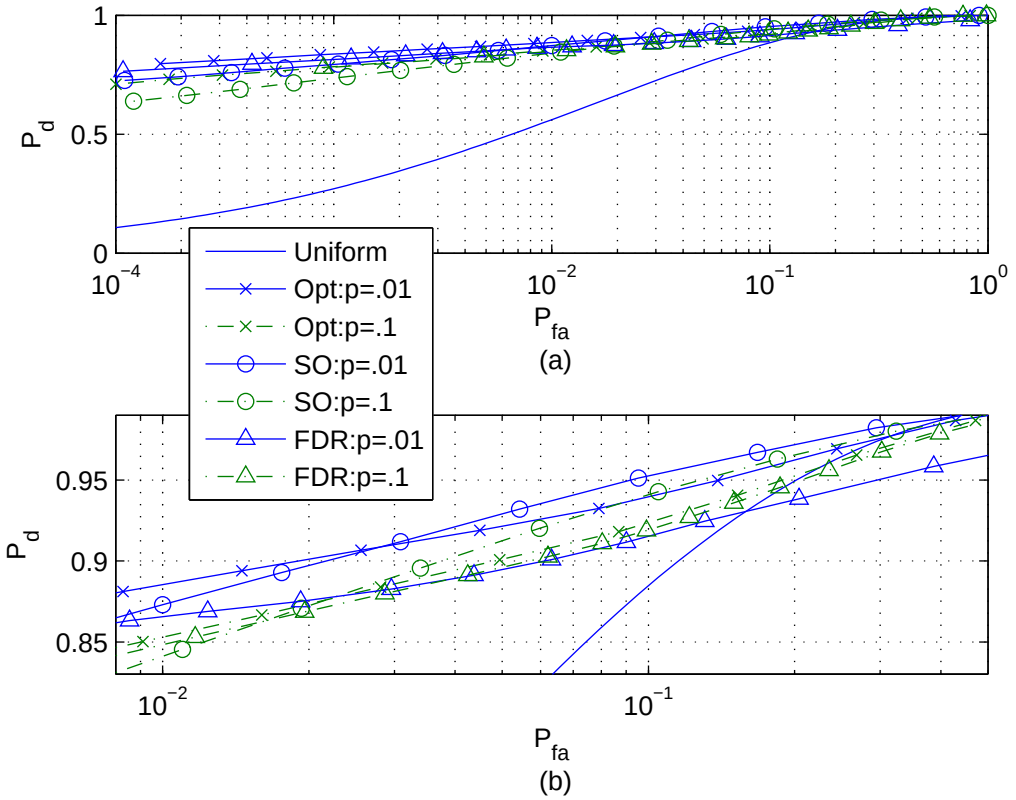

Fig. 4. We compare ROC curves for the LRT tests based on an exhaustive search scheme and the two adaptive policies measurements scheme using (69) and a FDR procedure, for $p = 0.1$ and $p = 0.01$ and SNR of 10 [dB]. (a) shows the entire ROC curve while (b) zooms in on false alarm probability values between 0.08 and 0.5. Our simulation result suggests that our adaptive search policies outperforms an exhaustive search policy in terms of detection probability for test values lower than 30%.

search, is the best that adaptive search can do for high false alarm probabilities (see discussion below). Two other things to notice: (i) Remarkably, minimizing the surrogate cost function (5) results in detection performance that are nearly optimal. (ii) By fixing $\nu = 1$ we do not lose a lot in terms of detection. Next we check the tradeoff between different ν values, detection probability and estimation MSE gain.

Finally we compare detection probability values, for a fixed false alarm rate, with estimation MSE gain as a function of ν. Results are shown in Figure 6. The curve with triangle markers on represent estimation MSE gain and its corresponding 'Y-axis' values are on the right hand side of the figure. The rest of the curves represent detection probability, as a function of ν, for a

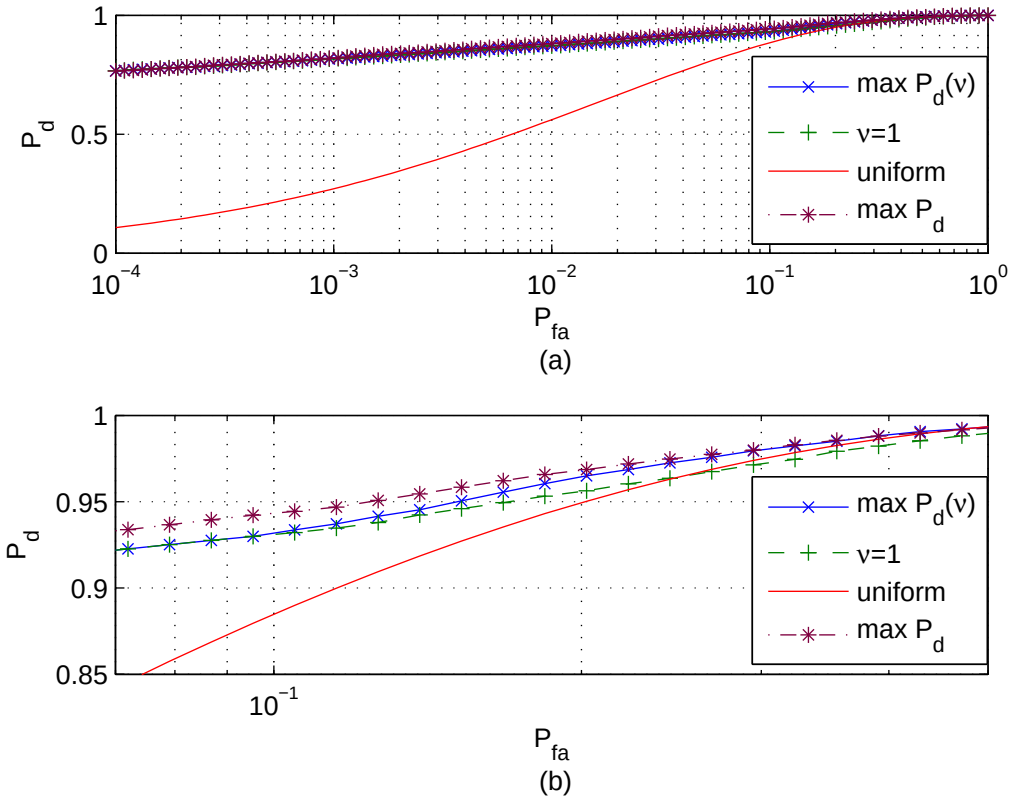

Fig. 5. We compare ROC curves for different tests. (a) shows the entire ROC curves while (b) focus on the area where the different curves crosses and merge. The solid with cross markers curve corresponding to the ν optimized detection test ('max $\mathrm{P_d}(\nu)$') does not significantly outperform the dashed curve with plus markers, which is due to choosing $\nu = 1$, for small false alarm probability values. Moreover, the 'envelope' curve is very similar to the detection optimized test curve (dashed-dotted with asterisks), suggesting that minimizing our cost function provides a near optimal detection performances.

given test level, with the corresponding 'Y-axis' values at the left hand side. For the selected operating point it is clear that it is best to choose $\nu = 1$ (or very close to 1), since it maximizes both detection and estimation performance.

D. Discussion

The following may help understand the nature of the optimal adaptive search algorithm, when $\nu = 1$. At the first step, the entire medium is scanned with some energy to generate a posterior distribution. At which point inequality (38) yields a specific k_0. This k_0 dictates the cardinality of the intermittent estimated ROI, $\widehat{\Psi}$. If $k_0 = 0$, then $\widehat{\Psi} = \mathcal{X}$ and all Q cells are in $\widehat{\Psi}$. However,

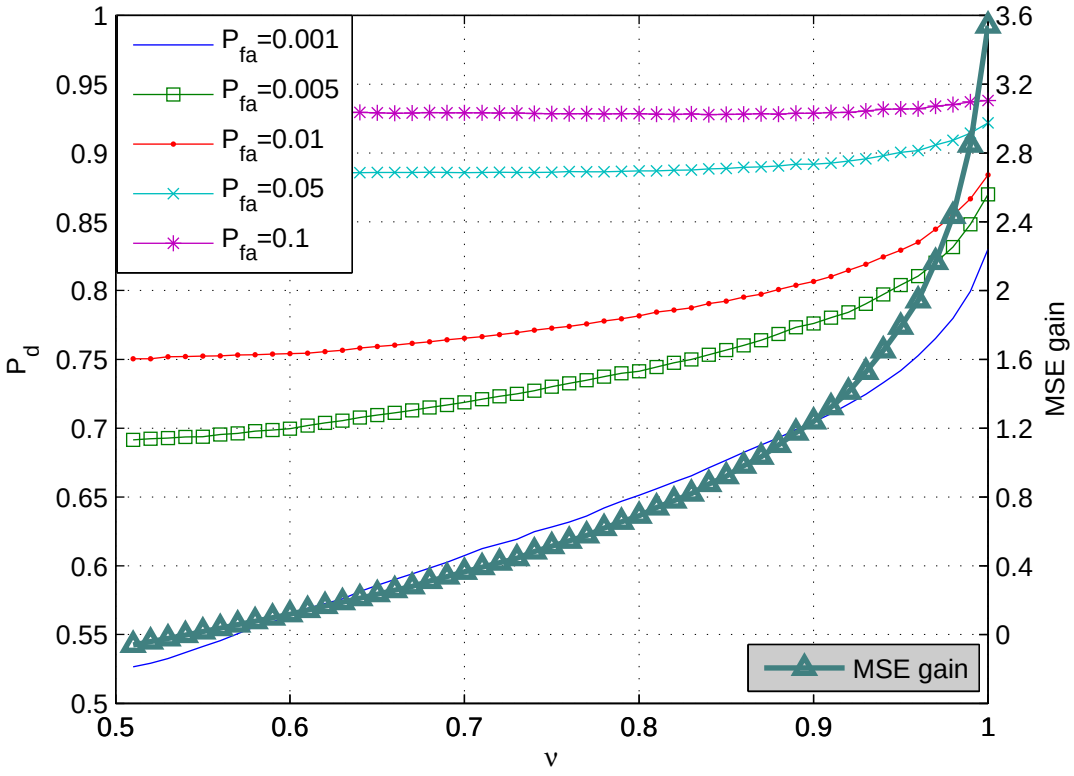

Fig. 6. We compare detection probability, for a fixed test level, and estimation MSE gain as a function of ν when SNR is 10 [dB] and $p = 0.01$. Note that the MSE gain values (curve with triangular markers) are given on the r.h.s. of the figure. Since MSE gain is defined over the true ROI it increases with ν.

$\Pr(k_0 > 0)$ increases with Q and SNR, and as was shown in section III-B1, at high SNR $\mathrm{E}\{k_0\} \rightarrow (1-p)Q$. As soon as $k_0 \neq 0$ cells are being excluded from the estimated ROI. The performance of our algorithm can be further explained using table I. The table entries are

TABLE I

POSSIBLE CELL COMBINATIONS

	Ψ	Ψ^c
$\widehat{\Psi}$	A	B
$\widehat{\Psi}^c$	C	D

formally defined as follows

$$\begin{aligned}
\mathrm{A} &= \{i : i \in (\Psi \cap \widehat{\Psi})\},\\
\mathrm{B} &= \{i : i \in (\Psi^c \cap \widehat{\Psi})\},\\
\mathrm{C} &= \{i : i \in (\Psi \cap \widehat{\Psi}^c)\},\\
\mathrm{D} &= \{i : i \in (\Psi^c \cap \widehat{\Psi}^c)\}.
\end{aligned}$$

Sets A and D correspond to the case where cells were correctly classified, after the first step, as belonging either to the true ROI, Ψ, or to its complement Ψ^c. Sets B represent false alarms, i.e., cells that were incorrectly detected as part of the true ROI, while group C represent miss detections. For estimation purposes it is best if B=C=$\emptyset$. This way all the remaining energy, at the second step, would be allocated to Ψ. This is not the case for detection though. Good detection performance requires that Ψ^c would be well characterized. An exhaustive search policy allocate most of the energy characterizing Ψ^c. In our case, group D is usually the largest, but the size of groups A, B, and C depends strongly on SNR. A large group B affects only estimation performance as some part of the remaining energy is invested at Ψ^c. On the other hand, a large group C affects both estimation and detection performances. Cells in group C are only probed at the first step, and with less energy compared to what is used in an exhaustive search. Therefore it is: a) hard to estimate the true value of those cells b) any test performed after the second step has a hard task trying to classify them correctly.

V. Application - detecting and estimating a ROI in a SAR image

Consider the task of imaging a large area using a satellite equipped with a synthetic aperture radar (SAR) system. Assume we have satellite access at two different incidents each limited in time. In SAR imaging the measurements quality improves as the dwell time increases. Therefore, with limited access to satellite time we face the question of how to best utilize the resource available to us, i.e., where and for how long to point the SAR system at each measurement. Assuming our goal is to detect and identify targets spread out in a large area we propose the following search policy based on *ARAP*: At first stage, use all the time available to perform an exhaustive search yielding a preliminary image or $\boldsymbol{y}(1)$ in *ARAP*. At second stage, let *ARAP* distribute the available time in a non uniform manner between different cells via (42), i.e., focusing the search on $\widehat{\Psi}$. Finally, we combine both measurements to form an image with non uniform spatial properties on which we detect the ROI and estimate its content. The competing

strategy performs an exhaustive search twice, with no adaptation between scans, than uses the arithmetic mean of the two independent scans as the estimated image.

We used a SAR image, taken from Sandia National Laboratories website[9] as an example of a "sparse" image. The image displays two columns of tanks in a field and its sparsity ratio $p < 0.01$. Let X denote the original image and let $\boldsymbol{x}$ be a lexicographic ordering of X. We emulated the effect of the SAR varying dwell time as modulated speckle noise variance in the post-processed SAR image. In particular, the SAR image after the first stage (equal dwell time at all pixels) is modeled as:

$$\boldsymbol{x}_1 = (1 + z_1)\boldsymbol{x}, \tag{70}$$

where z_1 is a zero mean uniform random variable with $\mathrm{var}(z_1) = \frac{1}{\lambda_0}$ noted as $z_1 \sim \mathrm{U}[-\sqrt{\frac{3}{\lambda_0}}, \sqrt{\frac{3}{\lambda_0}}]$. A tank template shown in Figure 7, was applied as a matched filter to the noisy image X_1 yielding $\widetilde{X}_1$. The input to our algorithm $\boldsymbol{y}(1) = \frac{\widetilde{\boldsymbol{x}}_1 - \overline{x}_1}{\sqrt{\frac{1}{Q}(\widetilde{\boldsymbol{x}}_1 - \overline{x}_1)'(\widetilde{\boldsymbol{x}}_1 - \overline{x}_1)}}$ was the normalized version of $\widetilde{X}_1$, where $\overline{x}_1 = \frac{1}{Q}\sum_{i=1}^{Q} \widetilde{\boldsymbol{x}}_1(i)$. *ARAP* was used to obtain a search policy for the second step $\lambda(i, 2)$ via (42). All indices i with $\lambda(i, 2) < \lambda_0$ were set to zero and their cumulative search effort was redistribute among the rest of the cells in a proportional manner. Next, $\boldsymbol{x}_2$ was generated via

$$\boldsymbol{x}_2 = (\boldsymbol{x} + \boldsymbol{x} \odot \boldsymbol{z}_2) \odot \boldsymbol{I}_{\widehat{\Psi}}, \tag{71}$$

where $z_2(i) \sim \mathrm{U}[0, \sqrt{\frac{12}{\lambda(i,2)}}]$ for all $i \in \widehat{\Psi}$ and zero otherwise, and $\odot$ denotes an element by element multiplication operator. Note that $\boldsymbol{x}_2 = 0$ for all $i \in \widehat{\Psi}^c$. We tried several suboptimal linear estimators based on $(\boldsymbol{x}_1, \boldsymbol{x}_2)$ and present here the one that performed best in terms of image 'quality'. The estimator $\widehat{X}$ was defined via $\widehat{\boldsymbol{x}}$ as

$$\widehat{\boldsymbol{x}} = \left(\frac{\boldsymbol{x}_1 \odot I\{i \in \widehat{\Psi}^c\}}{\sqrt{1 + 1/\lambda_1}} + \boldsymbol{x}_2 \odot \mathrm{vec}\left\{ \frac{1}{\sqrt{1 + 1/\lambda(i, 2)}} \right\} \right) \odot \boldsymbol{s}, \tag{72}$$

where $\mathrm{vec}\{r_i\} = [r_1, r_2, \ldots, r_Q]'$ and $\boldsymbol{s}(i) = \left(\sqrt{1 + \frac{1}{\lambda_1}} + \sqrt{1 + \frac{I\{i \in \widehat{\Psi}\}}{\lambda(i,2)}} \right)^{-1}$. The estimator (72) is compared to an image reconstructed from two exhaustive searches with equal effort allocation $(\boldsymbol{x}_{U1}, \boldsymbol{x}_{U2})$ given in (70), defined as $\boldsymbol{x}_U = (\boldsymbol{x}_{U1} + \boldsymbol{x}_{U2})/2$. SNR was defined as $10 \log 2\lambda_0$.

Results are presented in Figures 8 and 9 for SNR values of 4 and 0 [dB] respectively. Fig. 8(a) show the original image, Fig. 8(b) and (d) show a single realization of images reconstructed

[9]http://www.sandia.gov/RADAR/images/rtv_tanks_9in.jpg

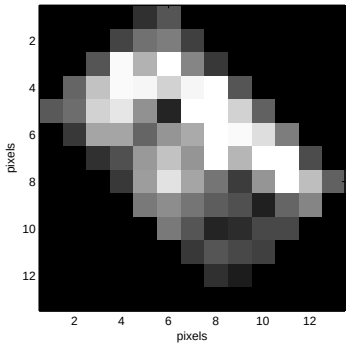

Fig. 7. The above (13×13) tank template was used as a matched filter to filter the noisy data X_1 and generate $\boldsymbol{y}(1)$.

using exhaustive search and *ARAP* via (72) respectively. Fig. 8(c) show the effort allocated by *ARAP* at the second stage for that specific realization. Although all targets are identifiable in Fig. 8(b) they seem clearer in Fig. 8(d). Figure 9 focus on the ROI to demonstrate the superiority of *ARAP* compared to an exhaustive search. Figures 9(a) and (b) show a single realization of the two search methods exhaustive and *ARAP* at 0 [dB] respectively, while Figs. 9(c) and (d) display a 1D profile, going through the left columns of tanks, of 100 different realizations of each policy respectively. It is evident that variations in profiles in images reconstructed using *ARAP* are much smaller than those in images resulted from an exhaustive search.

This illustrative example demonstrates a potential usage of our method to SAR imaging. Note that in the previous sections we had developed the problem in a context of energy allocation while we currently consider dwell time allocation as the resource at hand. We believe that our general framework is suitable for a variety of application including: medical imaging, target monitoring, and airport security screening by replacing 'energy' with the relevant resource.

VI. Conclusions and future work

We introduced a novel convex cost function and showed that minimizing it relates to minimizing error probability or estimation MSE over an unknown ROI. A closed form solution for the second step in a two-step optimal search policy was provided, and numeric search for the first step was presented. A closed form low complexity approximation for the two step minimization problem was also presented and it was shown to perform comparably to the optimal solution. In a high SNR the performance of the optimal and approximated algorithms was shown to converge to

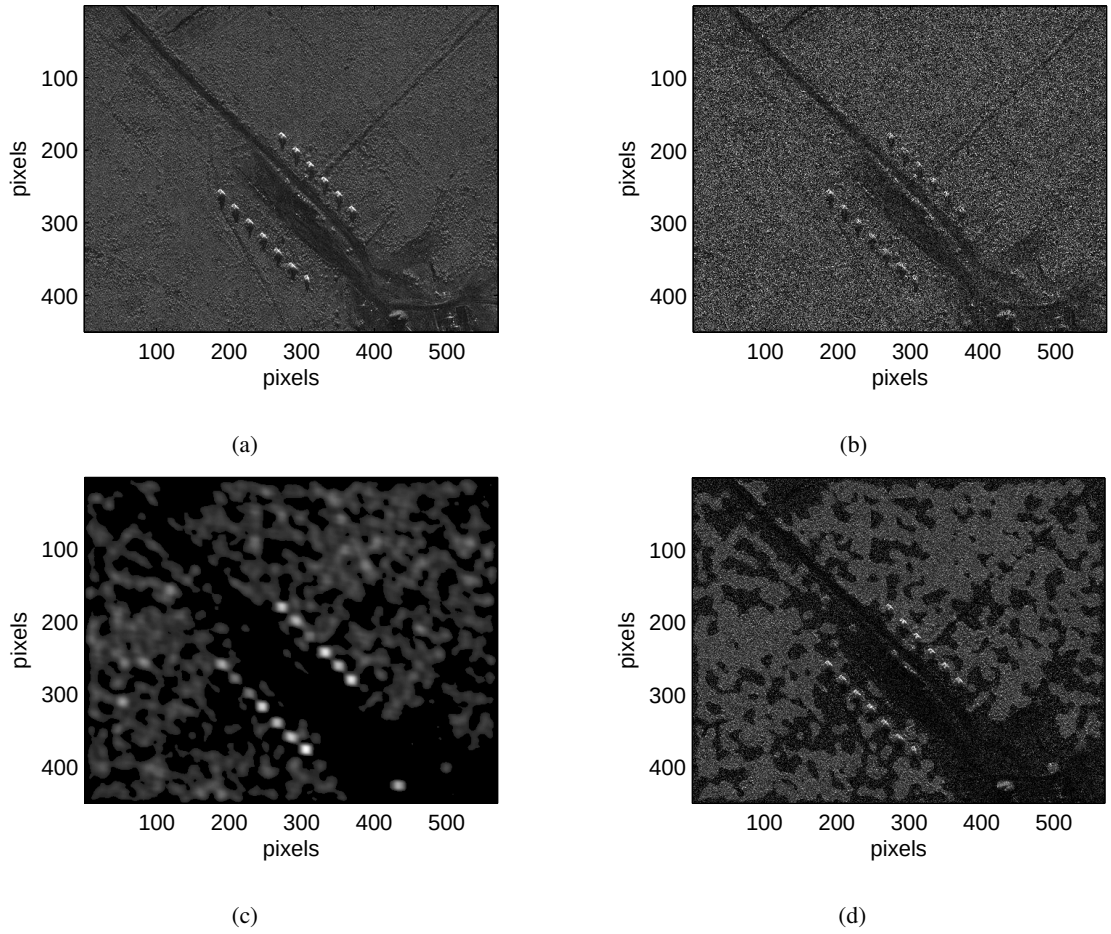

Fig. 8. SAR imaging example, SNR=4[dB]. (a) Original image. (b) Image reconstructed using two exhaustive searches. (c) Effort allocation using *ARAP* at the second stage. (d) Image resulted from (72) using *ARAP*.

the ideal omniscient limit. For the detection task, the two search policies introduced outperformed the one step exhaustive measurement scheme for false alarm values less than 30%. For estimation, comparing the MSE of estimated values within the ROI, our adaptive search policies dominate exhaustive search policy. The search policy is parameterized by ν which varies from $\frac{1}{2}$ to 1 and controls the energy allocated within the ROI. An offline lookup table can be generated for the optimal ν in terms of the sparseness p and SNR. Finally, an illustrative example of our method for SAR imaging was presented and potential benefits were discussed.

This approach is applicable to tumor detection where a cluster of calcification may appear around the lesion. In this case multiscale hypothesis testing methods presented in [34] may be relevant. [34] deals with anomaly detection once measurements, at a fine resolution, have

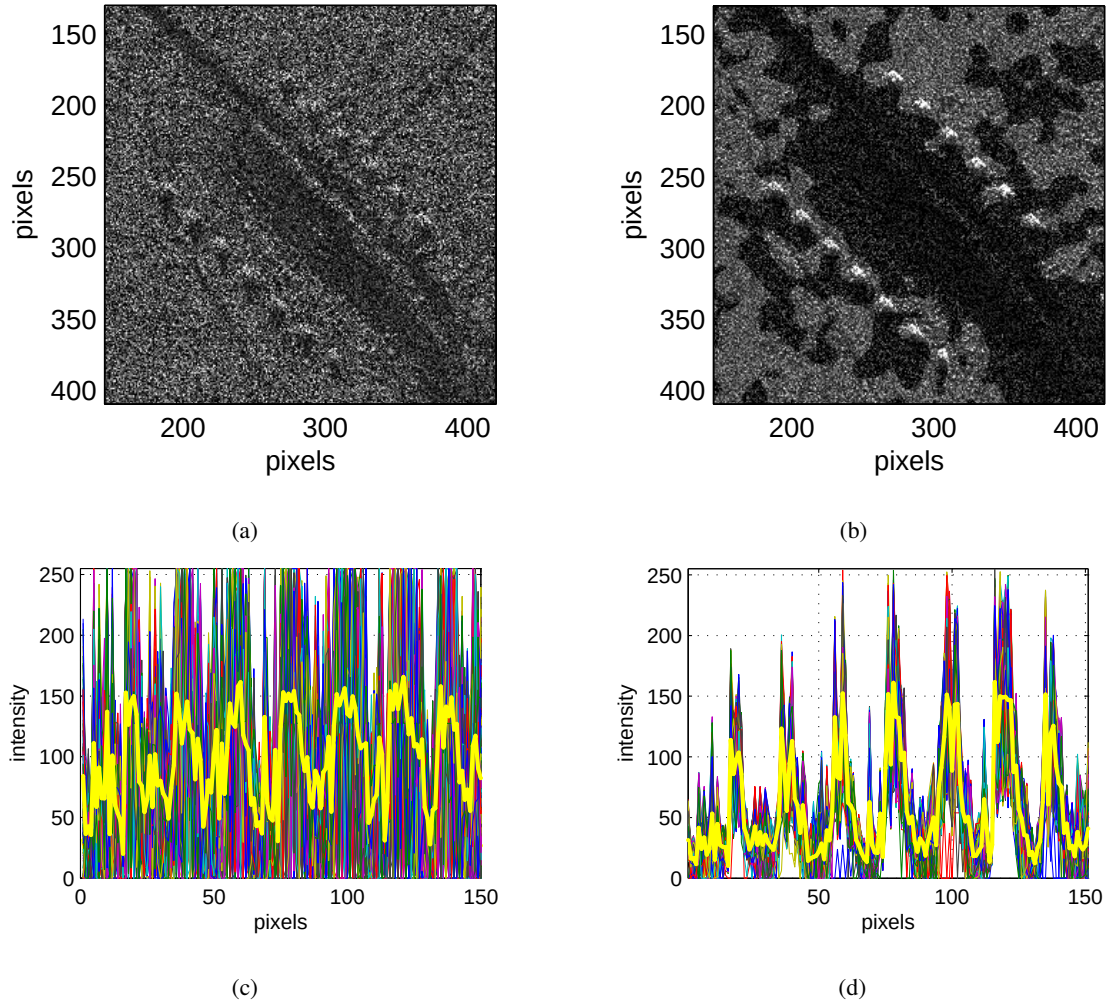

Fig. 9. SAR imaging example, SNR=0[dB]. (a) Image reconstructed using two exhaustive searches, targets are not easily identifiable. (b) Image resulted from (72) using *ARAP*. Figures (c) and (d) compare a 1D profile going through the targets on the lower left column for 100 different realizations. (c) Profiles of images reconstructed from an exhaustive search. (d) Profiles of images reconstructed using *ARAP*. The bold bright line on both figures represent the mean profile of the different realizations. Evidently, variations of profiles of images due to *ARAP* are much smaller compared to variations of profiles of images resulted from an exhaustive scan.

been acquired. Our goal is to generate fine resolution measurements only where it is necessary. Another interesting area of application is to compressive sensing. Work such as [35] and [36] consider the problem of sampling a sparse medium via an arbitrary affine transformation. In cases of sparse signals complete reconstruction of the underlying signal can be accomplished with only a few samples. This exploitation of sparsity is analogous to the methods proposed in this report.

ACKNOWLEDGEMENT

This work was supported in part by AFOSR MURI under Grant FA9550-06-1-0324.

APPENDIX I

EQUIVALENCY OF MINIMIZING OUR COST TO MINIMIZING THE *Cramér-Rao* BOUND

Consider the problem of estimating an unknown signal in the presence of a Gaussian noise. Let $\boldsymbol{y}_{m\times 1}$ be a measurements vector given by

$$\boldsymbol{y} = \text{diag}\{\sqrt{\boldsymbol{\lambda}}\}\boldsymbol{\mu} + \boldsymbol{n}, \tag{73}$$

where $\boldsymbol{n} \sim \mathcal{N}(\mathbf{0}, \sigma^2\text{I})$. Let Ψ be a collection of indices, namely the ROI, with $|\Psi| \ll m$. Assume that the effort to be distributed is the measurement energy λ_i associated with measuring an element of $\boldsymbol{y}$, with $\sum_i \lambda_i = 1$. Define $z_i = \frac{y_i}{\sqrt{\lambda_i}}$, hence

$$z_i \sim \mathcal{N}\left(\mu_i, \frac{\sigma^2}{\lambda_i}\right). \tag{74}$$

Recall that the *Cramér-Rao* bound on the variance of any unbiased estimator $\hat{\mu}_i(z_i)$ of μ_i is given as

$$\text{VAR}(\hat{\mu}_i) \geqslant \frac{\sigma^2}{\lambda_i}, \tag{75}$$

which is also the measurement variance for this case. From (12) we know that the minimizer of our cost (5) when $\nu = 1$ is a uniform energy allocation within the ROI. Hence the optimal solution minimizing our cost $\lambda_i = \frac{1}{|\Psi|} I(i \in \Psi)$ also uniformly minimizes the *Cramér-Rao* bound on all $\hat{\mu}_i$ where $i \in \Psi$.

APPENDIX II

CHERNOFF BOUND ON THE PROBABILITY OF ERROR AND OUR COST FUNCTION

Let us consider simple binary, hypothesis testing problem of classifying an observation X as coming from one of two possible classes (hypotheses) H_0, H_1. Let π_0, π_1 denote the a priori probabilities on the hypotheses, and let $p_0(x), p_1(x)$ denote the conditional probability density functions given the true hypothesis. Then Bayes decision rule minimizes the probability of error P_e by choosing the hypothesis with the largest a posteriori probability. The Chernoff bound on P_e states that for any $\alpha \in [0, 1]$

$$P_e \leqslant \pi_0^{\alpha}\pi_1^{1-\alpha} \int_X [p_0(x)]^{\alpha} [p_1(x)]^{1-\alpha}\, dx. \tag{76}$$

Further let X be a Gaussian r.v. with known variance σ^2 and unknown mean with the two hypothesis corresponds to

$$\begin{array}{l} H_0 : \mu_0 = 0 \\ H_1 : \mu_1 > 0 \end{array}.$$

In this case (76) yields

$$P_e \leqslant \pi_0^{\alpha}\pi_1^{1-\alpha}\int \frac{1}{\sqrt{2\pi\sigma^2}} e^{-\frac{\alpha}{2\sigma^2}x^2} e^{-\frac{1-\alpha}{2\sigma^2}(x-\mu_1)^2} dx = \tag{77}$$

$$P_e \leqslant \pi_0^{\alpha}\pi_1^{1-\alpha}\int \frac{1}{\sqrt{2\pi\sigma^2}} e^{-\frac{1}{2\sigma^2}\left[\alpha x^2+(1-\alpha)(x^2-2\mu_1 x+\mu_1^2)\right]} dx = \tag{78}$$

$$P_e \leqslant \pi_0^{\alpha}\pi_1^{1-\alpha} e^{-\frac{\alpha(1-\alpha)\mu_1^2}{2\sigma^2}} \int \frac{1}{\sqrt{2\pi\sigma^2}} e^{-\frac{1}{2\sigma^2}\left[x^2-(1-\alpha)\mu_1\right]^2} dx, \tag{79}$$

and integration is over $(-\infty, \infty)$. Note that the integrand in the last equation is a Gaussian density, with mean $(1-\alpha)\mu_1$ and variance σ^2, that integrates to 1. Finally we get,

$$P_e \leqslant \pi_0^{\alpha}\pi_1^{1-\alpha} e^{-\frac{\alpha(1-\alpha)\mu_1^2}{2\sigma^2}}, \tag{80}$$

so the Chernoff bound on the probability of error, P_e, is a decreasing function of the unknown mean μ and an increasing function of the variance σ^2. Let $\boldsymbol{w}_{Q\times 1} \sim \mathcal{N}(\boldsymbol{\mu}, \sigma^2 \mathrm{I})$ and consider the problem of detecting between $\mu_i = 0$ and $\mu_i > 0$. Let $\Psi = \{i : \mu_i > 0\}$ and assume $|\Psi| \ll Q$. Further assume that by allocating energy $\lambda(i)$ to the i^{th} measurement we increase the *detectability index* $\frac{\mu_i}{\sigma}$, e.g. as in (20). For such a scenario, minimizing our cost function (5) with $\nu = 1$ results in uniformly allocating energy to all cells in Ψ. Utilizing (80) it implies uniformly minimizing P_e over Ψ.

APPENDIX III
SHOWING A GLOBAL LOWER BOUND ON OUR COST

In Section II we claimed that the r.h.s. of (6) is lower bounded by $|\Psi|^2$ for all $\nu \in [\frac{1}{2}, 1]$ and $\frac{|\Psi|}{Q} \leqslant \frac{1}{2}$. To prove this claim let $f(\nu) = [\sqrt{\nu}|\Psi| + \sqrt{1-\nu}(Q-|\Psi|)]^2$, then we need to show

$$f(\nu) \geqslant |\Psi|^2. \tag{81}$$

First note that

$$f(\frac{1}{2}) = \frac{Q^2}{2} > |\Psi|^2 = f(1), \tag{82}$$

since $\frac{|\Psi|}{Q} \leqslant \frac{1}{2}$. Next we show that $\dot{f}(\nu) \leqslant 0$ for all $\nu \in [\frac{1}{2}, 1]$, i.e., $f(\nu)$ is a decreasing function over the interval of interest. When combined with (82) this proves the claim. Note that

$$\dot{f}(\nu) = 2\left[\sqrt{\nu}|\Psi| + \sqrt{1-\nu}(Q-|\Psi|)\right]\left[\frac{|\Psi|}{\sqrt{\nu}} - \frac{Q-|\Psi|}{\sqrt{1-\nu}}\right], \tag{83}$$

hence it suffice to show

$$\left[\frac{|\Psi|}{\sqrt{\nu}} - \frac{Q-|\Psi|}{\sqrt{1-\nu}}\right] \leqslant 0. \tag{84}$$

Rearranging (84) we need to show

$$\sqrt{\frac{1-\nu}{\nu}} \leqslant \frac{Q-|\Psi|}{|\Psi|} = \frac{Q}{|\Psi|} - 1. \tag{85}$$

But $\nu \in [\frac{1}{2}, 1]$ provides $\frac{1-\nu}{\nu} \leqslant 1$, while $\frac{|\Psi|}{Q} \leqslant \frac{1}{2}$ results in $\frac{Q}{|\Psi|} - 1 \geqslant 1$ and hence the inequality in (85) holds. This completes the proof.

APPENDIX IV
SHOWING AN UPPER BOUND ON THE GAIN

Let I_i be a Bernoulli r.v. with $\Pr(I_i = 1) = p$. Define $|\Psi| = \sum_{i=1}^{Q} I_i$, then $|\Psi|$ is a Binomial r.v. and $|\Psi| \sim \mathrm{B}(p, Q)$. Further let $p^* = \frac{|\Psi|}{Q}$ then $\mathrm{E}\{p^*\} = p$ and $\mathrm{var}(p^*) = \frac{p(1-p)}{Q}$.

Claim 1: For an arbitrary effort allocation policy Λ and $\delta \geqslant \exp\{-Q\frac{3p}{8(1-p)}\}$ we have

$$\Pr(G(\Lambda) \leqslant -10\log p + \epsilon) \geqslant 1 - \delta, \tag{86}$$

where $\epsilon = -10\log\epsilon'$ and $\epsilon' < 1$ is the solution of

$$(1-\epsilon')^2 + (4-\epsilon')\frac{2}{3}\frac{1-p}{pQ}\ln\delta = 0. \tag{87}$$

Proof: For all Λ

$$J(\Lambda_o) \leqslant J(\Lambda), \tag{88}$$

and therefore

$$G(\Lambda) \leqslant G(\Lambda_o) = -10\log p^*, \tag{89}$$

thus

$$\Pr(G(\Lambda) \leqslant -10\log p + \epsilon) \geqslant \Pr(-10\log p^* \leqslant -10\log p + \epsilon), \tag{90}$$

for some $\epsilon > 0$. Next, we evaluate the expression on the r.h.s. of (90). Note that

$$\Pr(-10\log p^* \leqslant -10\log p + \epsilon) = \tag{91}$$

$$\Pr\left(\log p^* \geqslant \log p - \frac{\epsilon}{10}\right) = \tag{92}$$

$$\Pr\left(p^* \geqslant \frac{p}{10^{\frac{\epsilon}{10}}}\right) = \Pr(p^* \geqslant \epsilon' p) = 1 - \Pr(p^* \leqslant \epsilon' p), \tag{93}$$

where $\epsilon' = \frac{1}{10^{\frac{\epsilon}{10}}} < 1$. Note that

$$\Pr(p^* \leqslant \epsilon' p) = \Pr(p^* - p \leqslant p(\epsilon' - 1)) = \tag{94}$$

$$\Pr(p - p^* \geqslant p(1 - \epsilon')). \tag{95}$$

For a sequence of i.i.d. r.v.'s $\{X_i\}_{i=1}^n$ with $\mathrm{E}\{X_i\} = 0$, Bernstein's inequality provides

$$\Pr\left(\sum_{i=1}^{n} X_i \geqslant t\right) \leqslant \exp\left\{-\frac{t^2/2}{\sum_i \mathrm{E}X_i^2 + M\frac{t}{3}}\right\}, \tag{96}$$

for $t > 0$, and where $|X_i| \leqslant M$ with probability 1. Let $X_i = p - I_i$, then assuming $p \leqslant \frac{1}{2}$ yield $M = 1 - p$ and

$$\Pr(p - p^* \geqslant t) \leqslant \exp\left\{-\frac{Q\frac{t^2}{2}}{(1-p)\left(p + \frac{t}{3}\right)}\right\}. \tag{97}$$

Utilizing (97) we obtain

$$\Pr(p - p^* \geqslant p(1 - \epsilon')) \leqslant \exp\left\{-Q\frac{3}{2}\frac{p}{1-p}\frac{(1-\epsilon')^2}{4-\epsilon'}\right\} \triangleq \delta. \tag{98}$$

When combined, (90)-(98) provide

$$\Pr(G(\Lambda) \leqslant -10\log p + \epsilon) \geqslant 1 - \delta. \tag{99}$$

This completes the proof. ■

Discussion: Bernstein's inequality requires $t > 0$ which hold provided that $\epsilon' \in (0, 1)$. Unfortuntaely, this means that we do not have $\delta \to 0$ since substituting $\epsilon' = 0$ in (98) yields

$$\delta \geqslant \exp\left\{-Q\frac{3}{8}\frac{p}{1-p}\right\}, \tag{100}$$

and Q and p are given. Nevertheless, δ may still be sufficiently small to make *Claim 1* attractive. In Section V we provide a SAR imaging example of our methods. A $(450[\mathrm{pix}] \times 570[\mathrm{pix}])$ image containing 13 targets each roughly $(13[\mathrm{pix}] \times 13[\mathrm{pix}])$ is examined. This translates to $p < 0.01$ and $Q = 256,500$. Therefore, setting $\delta = 10^{-3}$ yields $\epsilon = 0.333$ or

$$\Pr(G(\Lambda) \leqslant -10\log p + 0.333) \geqslant 1 - 10^{-3},$$

i.e., the gain of any effort allocation policy Λ is smaller than 20.333[dB] with probability grater than 0.999.

APPENDIX V
MINIMIZING THE COST FUNCTION

Let $\boldsymbol{Y}(t) \in \mathcal{Y}$ be a $(Q \times 1)$ random vector (r.v.) with pdf $p_{\boldsymbol{Y}(t)}(\boldsymbol{y}) > 0$, for all $\boldsymbol{y} \in \mathcal{Y}$ and $t \in \{1, 2, \ldots, T\}$, representing random observations. Let $\boldsymbol{I}_\Psi = [I_1, I_2, \ldots, I_Q]'$ be a r.v. with $\Pr(I_i = 1) = p_i$. Let $Y_1^t = \{\boldsymbol{Y}(1), \boldsymbol{Y}(2), \ldots, \boldsymbol{Y}(t)\}$ be a collection of all observation up to time t. Define

$$x(i,t) : Y_1^{t-1} \to \mathbb{R}_+, \tag{101}$$

then, for some $\nu \in (\frac{1}{2}, 1]$, our goal is to find $\{\hat{x}(i,t)\}$ with $i = 1, \ldots, Q$ and $t = 1, \ldots, T$, such that

$$\hat{x}(i,t) = \arg\min_{x(i,t)} \mathrm{E}\left\{ \sum_{i=1}^{Q} \frac{\nu I_i + (1-\nu)(1-I_i)}{\sum_{t=1}^{T} x(i,t)} \right\}, \tag{102}$$

where expectation is taken w.r.t. $\boldsymbol{I}_\Psi$ and Y_1^{T-1}, subject to

$$\sum_{i=1}^{Q} \sum_{t=1}^{T} x(i,t) = X. \tag{103}$$

A. The case of $T = 1$

For $T = 1$, our cost function has the following form

$$\hat{x}(i) = \arg\min_{x(i)} \mathrm{E}\left\{ \sum_{i=1}^{Q} \frac{\nu I_i + (1-\nu)(1-I_i)}{x(i)} \right\}, \tag{104}$$

subject to $\sum_{i=1}^{Q} x(i) = X$, with the expectation taken w.r.t. $\boldsymbol{I}_\Psi$. Note that $\mathrm{E}\{I_i\} = p_i$, so $\hat{x}_i$ can be derived using Lagrange multiplier, i.e., finding the minimizer of

$$L(\boldsymbol{x}, \lambda) = \sum_{i=1}^{Q} \frac{\nu p_i + (1-\nu)(1-p_i)}{x(i)} + \lambda \left(\sum_{i=1}^{Q} x(i) - X \right). \tag{105}$$

Taking derivatives and setting them equal to zero, yields

$$\hat{x}(i) = \frac{X \sqrt{\nu p_i + (1-\nu)(1-p_i)}}{\sum_{j=1}^{Q} \sqrt{\nu p_j + (1-\nu)(1-p_j)}}. \tag{106}$$

B. The case of $T = 2$

Consider the following problem, given a set $\{c_i\}_{i=1}^{Q}$, where $c_i = x(i,1) > 0$ and $\sum_{i=1}^{Q} c_i = C$, our goal is minimize the cost, i.e., find

$$\hat{x}(i,2) = \arg\min_{x(i,2)} \mathrm{E} \sum_{i=1}^{Q} \frac{\nu I_i + (1-\nu)(1-I_i)}{c_i + x(i,2)}, \tag{107}$$

subject to

$$\sum_{i=1}^{Q} x(i,2) = X - C \geqslant 0, \tag{108}$$

and $x(i,2) : \boldsymbol{Y}(1) \to \mathbb{R}_+$. For brevity, let $x_i(\boldsymbol{Y}) = x(i,2)$, and note that in (107) expectation is taken w.r.t. $\boldsymbol{I}_\Psi$ and $\boldsymbol{Y}(1)$. Using iterated expectation, we obtain

$$\mathrm{E}\left\{ \sum_{i=1}^{Q} \frac{\nu I_i + (1-\nu)(1-I_i)}{c_i + x(i,2)} \right\} = \mathrm{E}\left\{ \sum_{i=1}^{Q} \mathrm{E}\left\{ \frac{\nu I_i + (1-\nu)(1-I_i)}{c_i + x_i(\boldsymbol{Y})} \middle| \boldsymbol{Y}(1) \right\} \right\}. \tag{109}$$

Given $\boldsymbol{Y}(1)$ the denominator is deterministic and expectation can be applied to the numerator, therefore (109) becomes

$$\mathrm{E}\left\{ \sum_{i=1}^{Q} \frac{\nu \mathrm{Pr}(I_i = 1|\boldsymbol{Y}(1)) + (1-\nu)(1 - \mathrm{Pr}(I_i = 1|\boldsymbol{Y}(1)))}{c_i + x_i(\boldsymbol{Y})} \right\}. \tag{110}$$

Define $p_{I_i|\boldsymbol{Y}} = \mathrm{Pr}(I_i = 1|\boldsymbol{Y}(1))$ and $W_i = \nu p_{I_i|\boldsymbol{Y}} + (1-\nu)(1-p_{I_i|\boldsymbol{Y}})$, we use Lagrange multiplier to minimize

$$\mathrm{E}\left\{ \sum_{i=1}^{Q} \frac{W_i}{c_i + x_i(\boldsymbol{Y})} \right\} + \int_{\mathcal{Y}} \lambda'(\boldsymbol{y}) \left(\sum_{i=1}^{Q} x_i(\boldsymbol{y}) - (X - C) \right) d\boldsymbol{y} = \tag{111}$$

$$\sum_{i=1}^{Q} \int_{\mathcal{Y}} \left[\frac{w_i}{c_i + x_i(\boldsymbol{y})} f_{\boldsymbol{Y}}(\boldsymbol{y}) + \lambda'(\boldsymbol{y}) \left(x_i(\boldsymbol{y}) - (X - C) \right) \right] d\boldsymbol{y}. \tag{112}$$

where $w_i = W_i(\boldsymbol{y})$ is a realization of the r.v. W_i. Since $f_{\boldsymbol{Y}}(\boldsymbol{y})$ is strictly positive, define $\lambda(\boldsymbol{y}) = \frac{\lambda'(\boldsymbol{y})}{f_{\boldsymbol{Y}}(\boldsymbol{y})}$, then, $\hat{x}_i$, the minimizer of (112) is also the minimizer of

$$\sum_{i=1}^{Q} \int_{\mathcal{Y}} \left[\frac{w_i}{c_i + x_i(\boldsymbol{y})} + \lambda(\boldsymbol{y}) x_i(\boldsymbol{y}) \right] d\boldsymbol{y}, \tag{113}$$

Note that our problem has translated to minimizing a separable sum of integrals of a positive integrands. Hence, finding

$$\hat{x}_i(\boldsymbol{Y}) = \arg\min_{x_i(\boldsymbol{Y})} \frac{w_i}{c_i + x_i(\boldsymbol{Y})} + \lambda(\boldsymbol{Y}) x_i(\boldsymbol{Y}), \tag{114}$$

suffice. Solving for $x_i(\boldsymbol{y})$ given the Lagrange multiplier $\lambda(\boldsymbol{Y})$ yields

$$x_i(\boldsymbol{Y}) = \begin{cases} \sqrt{\frac{w_i}{\lambda(\boldsymbol{Y})}} - c_i, & \sqrt{\frac{w_i}{\lambda(\boldsymbol{Y})}} > c_i \\ 0, & \text{Otherwise} \end{cases}, \tag{115}$$

which can be also written as

$$x_i(\boldsymbol{Y}) = \left(\sqrt{\frac{w_i}{\lambda(\boldsymbol{Y})}} - c_i\right) I\left(\lambda(\boldsymbol{Y}) < \frac{w_i}{c_i^2}\right), \tag{116}$$

where $I(\cdot)$ is an indicator function. Utilizing the constraint $\sum_i x_i(\boldsymbol{Y}) = X - C$, we obtain

$$\frac{1}{\sqrt{\lambda(\boldsymbol{Y})}} \sum_{i=1}^{Q} \sqrt{w_i} I\left(\lambda(\boldsymbol{Y}) < \frac{w_i}{c_i^2}\right) = X - \left(C - \sum_{i=1}^{Q} c_i I\left(\lambda(\boldsymbol{Y}) < \frac{w_i}{c_i^2}\right)\right). \tag{117}$$

Note that

$$C = \sum_{i=1}^{Q} c_i I\left(\lambda(\boldsymbol{Y}) < \frac{w_i}{c_i^2}\right) + \sum_{i=1}^{Q} c_i I\left(\lambda(\boldsymbol{Y}) \geqslant \frac{w_i}{c_i^2}\right), \tag{118}$$

substituting (118) into (117) and rearranging, yields

$$\sqrt{\lambda(\boldsymbol{Y})} = \frac{\sum_{i=1}^{Q} \sqrt{w_i} I\left(\lambda(\boldsymbol{Y}) < \frac{w_i}{c_i^2}\right)}{X - \sum_{i=1}^{Q} c_i I\left(\lambda(\boldsymbol{Y}) \geqslant \frac{w_i}{c_i^2}\right)}. \tag{119}$$

Next, use $\tau : \mathcal{X} \to \mathcal{X}$ such that

$$z_{\tau(1)} \leqslant z_{\tau(2)} \leqslant \ldots \leqslant z_{\tau(Q)}, \tag{120}$$

where $z_{\tau(i)} = \frac{w_{\tau(i)}}{c_{\tau(i)}^2}$.,

1) Case $\lambda(\boldsymbol{Y}) < z_{\tau(1)}$: If $\lambda(\boldsymbol{Y}) < z_{\tau(1)}$, for all $\boldsymbol{Y}$, then $\lambda(\boldsymbol{Y}) < z_{\tau(i)}$ for all i and

$$\sqrt{\lambda(\boldsymbol{Y})} = \frac{\sum_{i=1}^{Q} \sqrt{w_{\tau(i)}}}{X}. \tag{121}$$

For which case, the cost minimizer is achieved at

$$x_{\tau(i)}(\boldsymbol{Y}) = \frac{X\sqrt{w_{\tau(i)}}}{\sum_{j=1}^{Q} \sqrt{w_j}} - c_{\tau(i)}, \tag{122}$$

and, for all i

$$\frac{X}{c_{\tau(i)}} \geqslant \frac{\sum_{j=1}^{Q} \sqrt{w_j}}{\sqrt{w_{\tau(i)}}}. \tag{123}$$

2) Case $\lambda(\boldsymbol{Y}) \geqslant z_{\tau(Q)}$: For the other extreme, we have $\lambda(\boldsymbol{Y}) \geqslant z_{\tau(i)}$ for all i, which in turn provides $\lambda(\boldsymbol{Y}) = 0$, due to (119). This can only hold if both $\nu = 1$ and $p_{I_i|\boldsymbol{Y}} = 0$ for all i. If this is the case, then for any choice of $x_i(\boldsymbol{Y})$ the overall cost is zero.

3) Case $z_{\tau(k)} \leqslant \lambda(\boldsymbol{Y}) < z_{\tau(k+1)}$, for some $k \in \{1, 2, \ldots, Q-1\}$: The interesting case is when $\lambda(\boldsymbol{Y})$ has some intermittent value, i.e.,

$$\sqrt{z_{\tau(k)}} \leqslant \frac{\sum_{i=k+1}^{Q} \sqrt{w_{\tau(i)}}}{X - \sum_{i=1}^{k} c_{\tau(i)}} < \sqrt{z_{\tau(k+1)}}. \tag{124}$$

Since all the terms in (124) are positive, we rewrite the inequality as

$$\frac{c_{\tau(k+1)} \sum_{i=k+1}^{Q} \sqrt{w_{\tau(i)}}}{\sqrt{w_{\tau(k+1)}}} + \sum_{i=1}^{k} c_{\tau(i)} < X \leqslant \frac{c_{\tau(k)} \sum_{i=k+1}^{Q} \sqrt{w_{\tau(i)}}}{\sqrt{w_{\tau(k)}}} + \sum_{i=1}^{k} c_{\tau(i)}. \tag{125}$$

Define

$$\begin{aligned} \mathrm{LB}(k) &= \tfrac{c_{\tau(k+1)} \sum_{i=k+1}^{Q} \sqrt{w_{\tau(i)}}}{\sqrt{w_{\tau(k+1)}}} + \textstyle\sum_{i=1}^{k} c_{\tau(i)}, \\ \mathrm{UB}(k) &= \tfrac{c_{\tau(k)} \sum_{i=k+1}^{Q} \sqrt{w_{\tau(i)}}}{\sqrt{w_{\tau(k)}}} + \textstyle\sum_{i=1}^{k} c_{\tau(i)}. \end{aligned} \tag{126}$$

To show that (125) makes sense, we need to show that for any X of interest there exists a unique $k = k_0 \in \{1, 2, \ldots, Q-1\}$ such that $X \in (\mathrm{LB}(k_0), \mathrm{UB}(k_0)]$. To do so we show that following: (i) $\mathrm{LB}(k) \leqslant \mathrm{UB}(k)$, (ii) $\mathrm{LB}(k-1) = \mathrm{UB}(k)$, and (iii) $X \in (\mathrm{LB}(Q-1), \mathrm{UB}(1)]$. Start with (i)

$$\frac{c_{\tau(k+1)} \sum_{i=k+1}^{Q} \sqrt{w_{\tau(i)}}}{\sqrt{w_{\tau(k+1)}}} + \sum_{i=1}^{k} c_{\tau(i)} - \left(\frac{c_{\tau(k)} \sum_{i=k+1}^{Q} \sqrt{w_{\tau(i)}}}{\sqrt{w_{\tau(k)}}} + \sum_{i=1}^{k} c_{\tau(i)} \right) = \tag{127}$$

$$\left(\frac{c_{\tau(k+1)}}{\sqrt{w_{\tau(k+1)}}} - \frac{c_{\tau(k)}}{\sqrt{w_{\tau(k)}}} \right) \sum_{i=k+1}^{Q} \sqrt{w_{\tau(i)}} = \left(\frac{\sqrt{z_{\tau(k)}} - \sqrt{z_{\tau(k+1)}}}{\sqrt{z_{\tau(k)} z_{\tau(k+1)}}} \right) \sum_{i=k+1}^{Q} \sqrt{w_{\tau(i)}} \leqslant 0, \tag{128}$$

since $z_{\tau(k)} \leqslant z_{\tau(k+1)}$. Note that $z_{\tau(k)} = z_{\tau(k+1)}$ implies that the interval $(\mathrm{LB}(k), \mathrm{UB}(k)]$ is empty. To prove (ii) we substitute $(k-1)$ for k in the expression for $\mathrm{LB}(k)$ in (126). This yields

$$\mathrm{LB}(k-1) - \mathrm{UB}(k) = \tag{129}$$

$$\frac{c_{\tau(k)} \sum_{i=k}^{Q} \sqrt{w_{\tau(i)}}}{\sqrt{w_{\tau(k)}}} + \sum_{i=1}^{k-1} c_{\tau(i)} - \left(\frac{c_{\tau(k)} \sum_{i=k+1}^{Q} \sqrt{w_{\tau(i)}}}{\sqrt{w_{\tau(k)}}} + \sum_{i=1}^{k} c_{\tau(i)} \right) = \tag{130}$$

$$\frac{c_{\tau(k)} \sum_{i=k}^{Q} \sqrt{w_{\tau(i)}}}{\sqrt{w_{\tau(k)}}} - \frac{c_{\tau(k)} \sum_{i=k+1}^{Q} \sqrt{w_{\tau(i)}}}{\sqrt{w_{\tau(k)}}} - c_{\tau(k)} = 0. \tag{131}$$

Combining (i) and (ii) we obtain

$$\mathrm{LB}(k) \leqslant \mathrm{UB}(k) = \mathrm{LB}(k-1), \tag{132}$$

i.e., $\mathrm{LB}(k)$ is decreasing in k. Finally, we need to show

$$X \in (\mathrm{LB}(Q-1), \mathrm{UB}(1)]. \tag{133}$$

From (126) we obtain

$$\mathrm{LB}(Q-1) = \sum_{i=1}^{Q} c_i. \tag{134}$$

If $\sum_i c_i = X$ then $x_i(\boldsymbol{Y}) = 0$, for all i, due to the constraint (108). Thus, for a two-step problem we must have $X > \sum_i c_i = \mathrm{LB}(Q-1)$. In addition (126) provides

$$\mathrm{UB}(1) = c_{\tau(1)} \sum_{i=1}^{Q} \sqrt{\frac{w_{\tau(i)}}{w_{\tau(1)}}}. \tag{135}$$

However, if $X > \mathrm{UB}(1)$, then from (123) we know that this corresponds to the case $\lambda(\boldsymbol{Y}) < z_{\tau(1)}$, for which we had already derived a solution. Together (i), (ii), and (iii) proves existence and uniqueness of the solution, since

1. $X \in (\mathrm{LB}(Q-1), \mathrm{UB}(1)]$,
2. $\bigcup_{k=1}^{Q} (\mathrm{LB}(k), \mathrm{UB}(k)] = (\mathrm{LB}(Q-1), \mathrm{UB}(1)]$,
3. $(\mathrm{LB}(i), \mathrm{UB}(i)] \cap (\mathrm{LB}(j), \mathrm{UB}(j)] = \emptyset, \ \forall i \neq j$.

To conclude this section we provide the following algorithm to find, $\hat{x}_i(\boldsymbol{Y})$, the minimizer of (107);

Algorithm 2: Step two minimizer

(i) For a given $\boldsymbol{Y}$, if $X >$UB(1), then $k_0 = 0$, else k_0 is the unique solution of (125).

(ii) For $k_0 \in \{0, 1, \ldots, Q-1\}$ the cost minimizer is achieved at

$$x_{\tau(i)}(\boldsymbol{Y}) = \left(\frac{X - \sum_{j=1}^{k_0} c_{\tau(j)}}{\sum_{j=k_0+1}^{Q} \sqrt{w_{\tau(j)}}} \sqrt{w_{\tau(i)}} - c_{\tau(i)} \right) I(i > k_0). \tag{136}$$

Note that this is the optimal solution given the set $\{c_i\}_{i=1}^{Q}$. To derive a two step optimal effort allocation scheme one has to specify the set $\{c_i\}_{i=1}^{Q}$. In general, this involves a $Q+1$ degrees of freedom grid search and is not feasible for large Q. Nevertheless, one can derive a suboptimal solution for any given prior probabilities $\{p_i\}$ using the following myopic approach: (i) Start with distributing the total effort to the two steps as $(\alpha X, (1-\alpha)X)$, with $\alpha \in (0,1)$. (ii) Distribute effort optimally, within each step, according to (106) and (136). (iii) Grid search over α to find the optimal effort allocation between the two steps.

C. The case of $T > 2$

For $T > 2$, we first find $\hat{x}(i,T)$ the minimizer of the last step, then use a backward induction to find $\hat{x}(i,t)$, for $t < T$. First, define

$$X^{(t)} = \sum_{i=1}^{Q} x(i,t), \tag{137}$$

with $\sum_{t=1}^{T} X^{(t)} = X$. Next, rewrite (107) as

$$\hat{x}(i,T) = \arg\min_{x(i,T)} \mathrm{E}\left\{ \sum_{i=1}^{Q} \frac{\nu I_i + (1-\nu)(1-I_i)}{c_i + x(i,T)} \right\}, \tag{138}$$

where

$$c_i = \sum_{t=1}^{T-1} x(i,t), \tag{139}$$

with $\sum_i c_i = C = \sum_{t=1}^{T-1} X^{(t)}$, subject to

$$\sum_{i=1}^{Q} x(i,T) = X - C > 0, \tag{140}$$

and $x(i,T) : Y_1^{T-1} \to \mathbb{R}_+$. Let $x_i(\boldsymbol{Y}) = x(i,T)$, and note that in (138) expectation is taken w.r.t. $\boldsymbol{I}_\Psi$ and Y_1^{T-1}. Using smoothing we get

$$\mathrm{E}\left\{ \sum_{i=1}^{Q} \frac{\nu I_i + (1-\nu)(1-I_i)}{c_i + x(i,2)} \right\} = \mathrm{E}_{Y_1^{T-1}}\left\{ \sum_{i=1}^{Q} \mathrm{E}\left\{ \frac{\nu I_i + (1-\nu)(1-I_i)}{c_i + x_i(\boldsymbol{Y})} \middle| Y_1^{T-1} \right\} \right\}, \tag{141}$$

and since, given Y_1^{T-1} the denominator is not random anymore, we get

$$\mathrm{E}\left\{ \sum_{i=1}^{Q} \frac{\nu I_i + (1-\nu)(1-I_i)}{c_i + x(i,2)} \right\} = \tag{142}$$

$$\mathrm{E}_{Y_1^{T-1}}\left\{ \sum_{i=1}^{Q} \frac{\nu \mathrm{Pr}(I_i = 1 | Y_1^{T-1}) + (1-\nu)(1 - \mathrm{Pr}(I_i = 1 | Y_1^{T-1}))}{c_i + x_i(\boldsymbol{Y})} \right\}. \tag{143}$$

Define $p_{I_i|\boldsymbol{Y}} = \mathrm{Pr}(I_i = 1 | Y_1^{T-1})$, we use Lagrange multiplier to minimize

$$L(\boldsymbol{x}, \lambda) = \sum_{i=1}^{Q} \left[\mathrm{E}_{Y_1^{T-1}}\left\{ \frac{w_i}{c_i + x_i(\boldsymbol{Y})} \right\} + \int_{\mathcal{Y}} \lambda'(\boldsymbol{Y}) x_i(\boldsymbol{Y}) d\boldsymbol{y} \right], \tag{144}$$

and, if $f_{Y_1^{T-1}}(\boldsymbol{y}) > 0$, then we can derive the exact same solution as in *algorithm 2*. To solve for $\hat{x}(i,t)$ for $t < T$, we define $c_i(t)$ as follows

$$c_i(t) = \sum_{j=1}^{t-1} x(i,j), \tag{145}$$

and solve

$$\hat{x}(i,t) = \arg\min_{x(i,t)} \mathrm{E}\left\{ \sum_{i=1}^{Q} \frac{\nu I_i + (1-\nu)(1-I_i)}{c_i + x(i,t)} \right\}, \tag{146}$$

subject to

$$\sum_{i=1}^{Q} x(i,t) = X^{(t)} - C \geqslant 0, \tag{147}$$

with $C = \sum_i c_i(t)$. Conditioning on the past and using Lagrange multiplier technique, we arrive again at a result similar to *algorithm 2*. The optimization problem translate to the following question, assuming we use the optimal mapping at each step how do we allocate $X^{(t)}$ for $t \in \{1, 2, \ldots, T\}$.

APPENDIX VI
CONVERGENCE OF $p_{I_i|\boldsymbol{y}(1)}$ FOR THE GAUSSIAN CASE

Consider a simplified version of the measurement model (20) given as

$$y_i(1) = \sqrt{\lambda_1} I_i \theta_i(1) + n_i(1), \tag{148}$$

where we substitute $t = 1$, $\lambda(i,1) = \lambda_1$, and $h_{ij}(1) = \delta_{ij}$ with δ_{ij} being the Kronecker delta. We further assume that the r.v. $\theta_i > 0$. For brevity we suppress the time dependency from here on. In addition we assumed $\Pr(I_i = 1) = p$ for all i and the noise samples are i.i.d. Gaussian with $n_i \sim \mathcal{N}(0, \sigma^2)$. Furthermore, setting $\varepsilon_i = \lambda_1$ for all i, results in i.i.d. measurements, distributed according to

$$y_i \sim \mathcal{N}(\sqrt{\lambda_1} I_i \theta_i, \sigma^2), \tag{149}$$

Therefore, the posterior probabilities $p_{I_i|\boldsymbol{y}}$ depends only on the i^{th} sample, i.e., $p_{I_i|\boldsymbol{y}} = p_{I_i|y_i}$. For the Gaussian case, $p_{I_i|y_i}$ has an explicit form given as

$$p_{I_i|y_i} = \frac{p \exp\{-\frac{1}{2\sigma^2}(y_i - \theta_i\sqrt{\lambda_1})^2\}}{p \exp\{-\frac{1}{2\sigma^2}(y_i - \theta_i\sqrt{\lambda_1})^2\} + (1-p)\exp\{-\frac{1}{2\sigma^2} y_i^2\}}, \tag{150}$$

which can be rearranged as

$$p_{I_i|y_i} = \frac{1}{1 + \frac{1-p}{p} \exp\left\{ -\frac{\theta_i \varepsilon_i}{\sigma^2} \left(\frac{y_i}{\sqrt{\lambda_1}} - \frac{\theta_i}{2} \right) \right\}}. \tag{151}$$

Let $z_i = \frac{y_i}{\sqrt{\lambda_1}}$, then $z_i \sim \mathcal{N}(\theta_i I_i, \eta^2)$ where $\eta^2 = \frac{\sigma^2}{\lambda_1}$ and at high SNR $\eta^2 \to 0$. Substituting y_i with z_i in (151) provides

$$p_{I_i|y_i} = p_{I_i|z_i} = \frac{1}{1 + \frac{1-p}{p} \exp\left\{-\frac{\theta_i}{\eta^2}\left(z_i - \frac{\theta_i}{2}\right)\right\}}. \tag{152}$$

Claim 2: The conditional probability $p_{I_i|y_i}$ defined in (152) converges in probability to I_i as $\eta \to 0$ for any $\theta_i > 0$, i.e., $\forall \epsilon > 0$ and some $\delta > 0$ there exists $\eta_0(\epsilon)$, such that $\forall \eta \leqslant \eta_0(\epsilon)$

$$\Pr(|p_{I_i|y_i}(\eta) - I_i| > \delta) \leqslant \epsilon, \tag{153}$$

The intuition behind *Claim 2* is derived from the following limit

$$\lim_{\eta^2 \to 0} p_{I_i|y_i} = \begin{cases} 0, & z_i < \frac{\theta_i}{2} \\ 1, & z_i > \frac{\theta_i}{2} \end{cases}. \tag{154}$$

Proof: Using Chebyshev's inequality we prove *Claim 2* for the case of $I_i = 0$. A symmetry argument suggests that the same line of proof can be applied for the case of $I_i = 1$. Define $A = \{z_i : z_i > \frac{\theta_i}{2}\}$ then

$$\Pr(|p_{I_i|y_i} - I_i| > \delta) = \Pr(A)\Pr(|p_{I_i|y_i} - I_i| > \delta|A) +$$
$$\Pr(A^c)\Pr(|p_{I_i|y_i} - I_i| > \delta|A^c). \tag{155}$$

For $I_i = 0$ we have[10]

$$\Pr(p_{I_i|y_i} > \delta) \leqslant \Pr(A) + \Pr\left(p_{I_i|y_i} > \delta \,\middle|\, z_i \leqslant \frac{\theta_i}{2}\right). \tag{156}$$

We show that both elements on the r.h.s. (156) approach zero as $\eta \to 0$. For some $\alpha > 0$, Chebyshev's inequality provides

$$\Pr\left(|z_i - \theta_i I_i| \geqslant \alpha\right) \leqslant \frac{\eta^2}{\alpha^2}. \tag{157}$$

Note that

$$\begin{aligned} &\Pr(z_i > \tfrac{\theta_i}{2}) \leqslant \Pr(|z_i - \theta_i I_i| \geqslant \tfrac{\theta_i}{2}), \quad I_i = 0, \\ &\Pr(z_i < \tfrac{\theta_i}{2}) \leqslant \Pr(|z_i - \theta_i I_i| \geqslant \tfrac{\theta_i}{2}), \quad I_i = 1, \end{aligned} \tag{158}$$

[10]Since $p_{I_i|y_i} \geqslant 0$ we can replace $p_{I_i|y_i} = |p_{I_i|y_i}|$.

and therefore

$$\Pr(A) \leqslant \Pr\left(|z_i| \geqslant \frac{\theta_i}{2}\right) \leqslant \frac{4\eta^2}{\theta_i^2}. \tag{159}$$

Next, we examine the term on r.h.s. of (156). Note that

$$\Pr\left(p_{I_i|y_i} > \delta \,\middle|\, z_i \leqslant \frac{\theta_i}{2}\right) = \tag{160}$$

$$\Pr\left(\frac{1}{1+\frac{1-p}{p}\exp\left\{\frac{\theta_i}{\eta^2}\left(\frac{\theta_i}{2}-z_i\right)\right\}} > \delta \,\middle|\, z_i \leqslant \frac{\theta_i}{2}\right) = \tag{161}$$

$$\Pr\left(\frac{\theta_i}{2} - z_i < \frac{\eta^2}{\theta_i}\ln\frac{p}{1-p}\frac{1-\delta}{\delta} \,\middle|\, z_i \leqslant \frac{\theta_i}{2}\right). \tag{162}$$

Let

$$\epsilon' = \frac{\eta^2}{\theta_i}\ln\frac{p}{1-p}\frac{1-\delta}{\delta}, \tag{163}$$

then (160) is equivalent to

$$\Pr\left(z_i \in \left[\frac{\theta_i}{2}-\epsilon', \frac{\theta_i}{2}\right]\right) \tag{164}$$

First, note that $\delta > p$ results in $\epsilon' < 0$ and hence (164) equals zero. Second, since $f_Z(z) \leqslant f_Z(0) = \frac{1}{\sqrt{2\pi\eta^2}}$ we have the following simple bound for any $\epsilon' > 0$

$$\Pr\left(z_i \in \left[\frac{\theta_i}{2}-\epsilon', \frac{\theta_i}{2}\right]\right) \leqslant \epsilon'\frac{1}{\sqrt{2\pi\eta^2}} = \eta\frac{1}{\theta_i\sqrt{2\pi}}\ln\frac{p}{1-p}\frac{1-\delta}{\delta}, \tag{165}$$

thus

$$\Pr\left(p_{I_i|y_i} > \delta \,\middle|\, z_i \leqslant \frac{\theta_i}{2}\right) \leqslant \eta\frac{1}{\theta_i\sqrt{2\pi}}\ln\frac{p}{1-p}\frac{1-\delta}{\delta}. \tag{166}$$

Finally, substituting (166) and (159) in (156) we obtain

$$\Pr(p_{I_i|y_i} > \delta) \leqslant \frac{4\eta^2}{\theta_i^2} + \eta\frac{1}{\theta_i\sqrt{2\pi}}\ln\frac{p}{1-p}\frac{1-\delta}{\delta}. \tag{167}$$

Define $\eta_0(\epsilon)$ as

$$\eta_0(\epsilon) = \sup_{\eta>0}\left\{\frac{4\eta^2}{\theta_i^2} + \eta\frac{1}{\theta_i\sqrt{2\pi}}\ln\frac{p}{1-p}\frac{1-\delta}{\delta} \leqslant \epsilon\right\}, \quad \forall\delta > 0, \tag{168}$$

then using (167) we have

$$p_{I_i|y_i} \to 0 \tag{169}$$

in probability when $I_i = 0$. In a similar manner, it can be shown that

$$p_{I_i|y_i} \to 1 \tag{170}$$

in probability for $I_i = 1$. ■

REFERENCES

[1] R. Castro, R. Willett, and R. Nowak, "Faster rates in regression via active learning," in *Advances in Neural Information Processing Systems 18*, Y. Weiss, B. Schölkopf, and J. Platt, Eds. Cambridge, MA: MIT Press, 2006, pp. 179–186.

[2] R. Nowak, U. Mitra, and R. Willett, "Estimating inhomogeneous fields using wireless sensor networks," *IEEE Journal on Selected Areas in Communication*, vol. 22, no. 6, pp. 999–1006, August 2004.

[3] R. Castro, R. Willet, and R. Nowak, "Coarse-to-fine manifold learning," in *Proceeding 2004 International Conference on Acoustics, Speech and Signal Processing*, vol. 3, May 2004, pp. iii–992–5.

[4] R. Willett, A. Martin, and R. Nowak, "Backcasting: adaptive sampling for sensor networks," in *Third International Symposium on Information Processing in Sensor Networks*, April 2004, pp. 124–133.

[5] R. Castro, J. Haupt, and R. Nowak, "Compressed sensing vs. active learning," in *Proceeding 2006 International Conference on Acoustics, Speech and Signal Processing*, vol. 3, May 2006, pp. III–III.

[6] S. Mallat and Z. Zhang, "Matching pursuits with time-frequency dictionaries," *IEEE Transactions on Signal Processing*, vol. 41, no. 12, pp. 3397–3415, December 1995.

[7] I. Gorodnitsky and B. Rao, "Sparse signal reconstruction from limited data using focuss: a re-weighted minimum norm algorithm," *IEEE Transactions on Signal Processing*, vol. 45, no. 3, pp. 600–616, March 1997.

[8] M. Nafie, A. Tewfik, and M. Ali, "Deterministic and iterative solutions to subset selection problems," *IEEE Transactions on Signal Processing*, vol. 50, no. 7, pp. 1591–1601, July 2002.

[9] B. Wohlberg, "Noise sensitivity of sparse signal representations: reconstruction error bounds for the inverse problem," *IEEE Transactions on Signal Processing*, vol. 51, no. 12, pp. 3053–3060, December 2003.

[10] D. Malioutov, M. Cetin, and A. Willsky, "A sparse signal reconstruction perspective for source localization with sensor arrays," *IEEE Transactions on Signal Processing*, vol. 53, no. 8, pp. 3010–3022, August 2005.

[11] J. Tropp, "Just relax: convex programming methods for identifying sparse signals in noise," *IEEE Transactions on Information Theory*, vol. 52, no. 3, pp. 1030–1051, March 2006.

[12] O. D. Escoda, L. Granai, and P. Vandergheynst, "On the use of a priori information for sparse signal approximations," *IEEE Transactions on Signal Processing*, vol. 54, no. 9, pp. 3468–3482, September 2006.

[13] M. Aharon, M. Elad, and A. Bruckstein, "k-svd: An algorithm for designing overcomplete dictionaries for sparse representation," *IEEE Transaction Signal Processing*, vol. 54, no. 11, pp. 4311–4322, November 2006.

[14] R. Rangarajan, R. Raich, and A. O. Hero III, "Optimal experimental design for an inverse scattering problem," in *Proceedings. IEEE International Conference on Acoustics, Speech, and Signal Processing*, vol. 4, March 2005, pp. 1117–1120.

[15] ——, "Sequential design of experiments for a rayleigh inverse scattering problem," in *2005 IEEE/SP 13th Workshop on Statistical Signal Processing*, July 2005, pp. 625–630.

[16] ——, "Optimal sequential energy allocation for inverse problems," *IEEE Journal on Selected Topics in Signal Processing*, vol. 1, no. 1, pp. 67–78, June 2007.

[17] K. Kastella, "Discrimination gain to optimize detection and classification," *IEEE Transactions on Systems, Man and Cybernetics, Part A*, vol. 27, no. 1, pp. 112–116, January 1997.

[18] C. Kreucher, K. Kastella, and A. O. Hero III, "Sensor management using an active sensing approach," *Signal Processing*, vol. 85, no. 3, pp. 607–624, March 2005.

[19] ——, "Multitarget tracking using the joint multitarget probability density," *IEEE Transactions on Aerospace and Electronic Systems*, vol. 41, no. 4, pp. 1396–1414, October 2005.

[20] S. J. Benkoski, M. G. Monticino, and J. R. Weisinger, "A survey of the search theory literature," *Naval Research Logistics*, vol. 38, no. 4, pp. 469–494, 1991.

[21] E. Posner, "Optimal search procedures," *IEEE Transactions on Information Theory*, vol. 9, no. 3, pp. 157–160, July 1963.

[22] J. B. Kadane, "Optimal whereabouts search," *Operations Research*, vol. 19, pp. 894–904, July-August 1971.

[23] D. A. Castanon, "Optimal search strategies in dynamic hypothesis testing," *IEEE Transaction on Systems, Man and Cybernetics*, vol. 25, no. 7, pp. 1130–1138, July 1995.

[24] N.-O. Song and D. Teneketzis, "Discrete search with multiple sensors," *Mathematical Methods of Operations Research*, vol. 60, no. 1, pp. 1–13, September 2004.

[25] E. C. Fear, P. M. Meaney, and M. A. Stuchly, "Microwaves for breast cancer detection?" *IEEE Potentials*, vol. 22, no. 1, pp. 12–18, Febuary-March 2003.

[26] E. J. Bond, L. Xu, S. C. Hagness, and B. D. van Veen, "Microwave imaging via space-time beamforming for early detection of breast cancer," *IEEE Transactions on Antennas and Propagation*, vol. 51, no. 8, pp. 1690–1705, August 2003.

[27] L. Xu, S. K. Davis, S. C. Hagness, D. W. van der Weide, and B. D. van Veen, "Microwave imaging via space-time beamforming: experimental investigation of tumor detection in multilayer breast phantoms," *IEEE Transactions on Microwave Theory and Techniques*, vol. 52, no. 8, pp. 1856–1865, August 2004.

[28] L. Xu, E. J. Bond, B. D. van Veen, and S. C. Hagness, "An overview of ultra-wideband microwave imaging via space-time beamforming for early-stage breast-cancer detection," *IEEE Antennas and Propagation Magazine*, vol. 47, no. 1, pp. 19–34, Febuary 2005.

[29] S. K. Davis, H. Tandradinata, S. C. Hagness, and B. D. van Veen, "Ultrawideband microwave breast cancer detection: a detection-theoretic approach using the generalized likelihood ratio test," *IEEE Transaction on Biomedical Engineering*, vol. 52, no. 7, pp. 1237–1250, July 2005.

[30] Cover, Thomas M. and Thomas, Joy A. , *Elements of information theory*. New York, NY, USA: Wiley-Interscience, 1991.

[31] W. Buntine, "Learning classification rules using bayes," in *Proceedings of the sixth international workshop on Machine learning*. San Francisco, CA, USA: Morgan Kaufmann Publishers Inc., 1989, pp. 94–98.

[32] S. M. Kay, *Fundamentals of Statistical Signal Processing, Volume 2: Detection Theory*. Prentice-Hall PTR, January 1998.

[33] Y. Benjamini and Y. Hochberg, "Controlling the false discovery rate: A practical and powerful approach to multiple testing," *Journal of the Royal Statistical Society. Series B (Methodological)*, vol. 57, no. 1, pp. 289–230, 1995.

[34] A. B. Frakt, W. C. Karl, and A. S. Willsky, "A multiscale hypothesis testing approach to anomaly detection and localization from noisy tomographic data," *IEEE Transactions on Image Processing*, vol. 7, no. 6, pp. 825–837, June 1998.

[35] M. B. Wakin, J. N. Laska, M. F. Duarte, D. Baron, S. Sarvotham, D. Takhar, K. F. Kelly, and R. G. Baraniuk, "An architecture for compressive imaging," in *IEEE International Conference on Image Processing*, October 2006, pp. 1273–1276.

[36] M. B. Wakin and R. G. Baraniuk, "Random projections of signal manifolds," in *Proceedings IEEE Conference on Acoustics, Speech and Signal Processing*, vol. 5, May 2006, pp. V–V.